

Scaling picture of magnetism formation in the anomalous f -electron systems: Interplay of the Kondo effect and spin dynamics

V. Yu. Irkhin and M. I. Katsnelson*

Institute of Metal Physics, 620219 Ekaterinburg, Russia

(Received 27 December 1996; revised manuscript received 15 May 1997)

The formation of a magnetically ordered state in the Kondo lattice is treated within the degenerate $s-f$ exchange and Coqblin-Schrieffer models. The Kondo renormalizations of the effective coupling parameter, magnetic moment, and spin-excitation frequencies are calculated within perturbation theory. The results of lowest-order-scaling consideration of the magnetic state in the Kondo lattices are analyzed. The dependence of the critical values of bare model parameters on the type of magnetic phase and space dimensionality is investigated. Renormalization of the effective Kondo temperature by interatomic exchange interactions is calculated. An important role of the character of spin dynamics (existence of well-defined magnon excitations) is demonstrated. The regime of strongly suppressed magnetic moments, which corresponds to magnetic heavy-fermion system, can occur in a rather narrow parameter region only. At the same time, in the magnetically ordered phases the renormalized Kondo temperature depends weakly on the bare coupling parameter in some interval. The critical behavior, which corresponds to the magnetic transition with changing the bare $s-f$ coupling parameter, is investigated. In the vicinity of the strong-coupling regime the spectrum of the Bose excitations becomes softened. Thus, on the borderline of magnetic instability, the Fermi-liquid picture is violated in some temperature interval due to scattering of electrons by these bosons. This may explain the fact that a non-Fermi-liquid behavior often occurs in heavy-fermion systems near the onset of magnetic ordering. [S0163-1829(97)00437-2]

I. INTRODUCTION

Anomalous $4f$ and $5f$ compounds, including the Kondo lattice and heavy-fermion systems, were studied extensively starting from the middle of the 1980's.¹⁻³ From the very beginning of these investigations it became clear that the effects, connected with a regular arrangement of the Kondo centers (rare-earth or actinide ions), play a crucial role in the physics of such systems. When passing from one magnetic center to the Kondo lattice, two main features appear. First, provided that the strong-coupling regime takes place, the Abrikosov-Suhl resonance in the one-site t matrix leads to formation of a complicated band structure near E_F with a new energy scale (the Kondo temperature T_K) and sharp peaks and pseudogaps in the density of states.^{4,5} This provides a common explanation for the heavy-fermion behavior. Second, the competition between the Kondo screening of magnetic moments and intersite magnetic interactions is of great importance.^{6,5,4,7} Following the paper by Doniach,⁸ it was believed in early works that this competition leads to the total suppression of either magnetic moments or the Kondo anomalies. However, more recent experimental data and careful theoretical investigations made it clear that the Kondo lattices *as a rule* demonstrate magnetic ordering or are close to this. This concept was consistently formulated and justified in a series of papers.⁹⁻¹³ A very important circumstance is that interspin coupling between the Kondo sites results in smearing of singularities in electron and magnetic properties on a scale of the characteristic spin-dynamics frequency $\bar{\omega}$. On the other hand, $\bar{\omega}$ itself acquires renormalizations that result in a decrease of $\bar{\omega}$ due to the Kondo screening. A simple scaling consideration of this renormalization

process in the $s-f$ exchange model¹³ yields, depending on the values of bare parameters, both the "usual" states (a nonmagnetic Kondo lattice or a magnet with weak Kondo contributions) and a peculiar magnetic Kondo-lattice state. In the latter state, small variations of parameters lead to strong changes of the ground-state moment. Thus a characteristic feature of heavy-fermion magnets — high sensitivity of the ground-state moment to external factors like pressure and doping by a small amount of impurities — is naturally explained. At the same time, only the simplest $s-f$ model was considered in Ref. 13, and the equations obtained were not investigated in detail. Therefore a number of important features of the Kondo magnets were not described.

Recently, a number of anomalous f -electron systems ($U_xY_{1-x}Pd_3$, $UPt_{3-x}Pd_x$, $UCu_{5-x}Pd_x$, $CeCu_{6-x}Au_x$, $U_xTh_{1-x}Be_{13}$, etc.) demonstrating the so-called non-Fermi-liquid (NFL) behavior have become a subject of great interest (see, e.g., the reviews¹⁴). It should be noted that such a behavior is observed not only in alloys, but also in some stoichiometric compounds, e.g., Ce_7Ni_3 ,¹⁵ $CeCu_2Si_2$, $CeNi_2Ge_2$.¹⁶ These systems possess unusual logarithmic or power-law temperature dependences of electron and magnetic properties. It is a common practice to discuss such a behavior within the one-impurity two-channel Kondo model.¹⁷⁻¹⁹ However, the NFL behavior is typical for systems lying on the boundary of magnetic ordering and demonstrating strong spin fluctuations.¹⁴ So, many-center effects should play an important role in this phenomenon. On the other hand, for a number of anomalous f -electron systems like Sm_3Se_4 , Yb_4As_3 , as well as for the only "moderately heavy-fermion" d -electron system $Y_{1-x}Sc_xMn_2$, the heavy-fermion state itself seems to be connected with pecu-

liarities of intersite couplings (e.g., frustrations), rather than with the one-impurity Kondo effect.^{20,11,12} Thus the interplay of the Kondo effect and intersite spin dynamics results in a very rich and complicated picture rather than in the trivial mutual suppression.

The aim of the present paper is a systematic study of formation of the magnetic Kondo-lattice state and of its properties for various magnetic phases depending on the character of spin dynamics. In Sec. II we introduce main theoretical models which include orbital degeneracy and enable one to treat the Kondo effect for a lattice in different cases. In Sec. III we write down the scaling equations for the effective $s-f$ parameter and spin-fluctuation frequency (which plays the role of a cutoff for the Kondo divergences in concentrated f -electron systems). In Sec. IV the scaling approach for the ordered state is generalized by taking into account the renormalization of the residue of the spin Green's function at the magnon pole. The most simple large- N limit in the Coqblin-Schrieffer model where spin dynamics is unrenormalized is considered in Sec. V. The scaling picture for finite N is discussed in Sec. VI. In Sec. VII we discuss the critical behavior near the magnetic phase transition and discuss the possibility of the Fermi-liquid picture violation. The scaling behavior in the $s-f$ exchange model with a large orbital degeneracy is investigated in Sec. VIII and an explicit description of the non-Fermi-liquid behavior is obtained in this limiting case. In Appendix A we analyze the properties of the localized spin subsystem for the models under consideration in the absence of $s-f$ interaction. The Kondo renormalizations in the paramagnetic state with account of spin dynamics are considered in Appendix B. In Appendixes C and D we calculate the Kondo corrections to the electron spectrum (and thereby to the effective $s-f$ coupling) and spin-wave frequency in the magnetically ordered phases.

II. THEORETICAL MODELS

To treat the Kondo effect in a lattice we use the $s-d(f)$ exchange Hamiltonian

$$H = \sum_{\mathbf{k}\sigma} t_{\mathbf{k}} c_{\mathbf{k}\sigma}^{\dagger} c_{\mathbf{k}\sigma} + H_f + H_{sf} = H_0 + H_{sf}, \quad (1)$$

where $t_{\mathbf{k}}$ is the band energy. We consider the pure spin $s-d(f)$ exchange model with

$$H_f = \sum_{\mathbf{q}} J_{\mathbf{q}} \mathbf{S}_{-\mathbf{q}} \mathbf{S}_{\mathbf{q}}, \quad H_{sf} = - \sum_{\mathbf{k}\mathbf{k}'\alpha\beta} I_{\mathbf{k}\mathbf{k}'} \mathbf{S}_{\mathbf{k}-\mathbf{k}'} \boldsymbol{\sigma}_{\alpha\beta} c_{\mathbf{k}\alpha}^{\dagger} c_{\mathbf{k}'\beta}, \quad (2)$$

where \mathbf{S}_i and $\mathbf{S}_{\mathbf{q}}$ are spin operators and their Fourier transforms, $\boldsymbol{\sigma}$ are the Pauli matrices. For the sake of conveniently constructing the perturbation theory, we explicitly include the Heisenberg exchange interaction with the parameters $J_{\mathbf{q}}$ in the Hamiltonian, although in fact this interaction can be the indirect Ruderman-Kittel-Kasuya-Yosida (RKKY) coupling. Expanding the $s-d(f)$ matrix elements in the spherical functions yields

$$I_{\mathbf{k}\mathbf{k}'} = \sum_{lm} I_l Y_{lm}^*(\theta_{\mathbf{k}}, \phi_{\mathbf{k}}) Y_{lm}(\theta_{\mathbf{k}'}, \phi_{\mathbf{k}'}). \quad (3)$$

Hereafter we retain in Eq. (3) only one term $I_l \equiv I$ ($l=2$ for d electrons and $l=3$ for f electrons). Introducing the operators

$$c_{\mathbf{k}m\sigma} = i^l (4\pi)^{1/2} c_{\mathbf{k}\sigma} Y_{lm}(\theta_{\mathbf{k}}, \phi_{\mathbf{k}}), \quad (4)$$

which satisfy, after averaging over the angles of the vector \mathbf{k} , the Fermi commutation relations, we reduce H_{sf} to the form

$$H_{sf} = -I \sum_{\mathbf{k}\mathbf{k}'m\alpha\beta} \mathbf{S}_{\mathbf{k}-\mathbf{k}'} \boldsymbol{\sigma}_{\alpha\beta} c_{\mathbf{k}m\alpha}^{\dagger} c_{\mathbf{k}'m\beta}. \quad (5)$$

Assuming the electron and spin excitation spectrum to be isotropic, in final expressions for self-energies we can perform averaging over the angles of all the wave vectors and use the orthogonality relation

$$\int \int \sin\theta d\theta d\phi dY_{lm}^*(\theta, \phi) Y_{l'm'}(\theta, \phi) = \delta_{mm'}.$$

Thus the factors of $[l] = (2l+1)$ occur in any order of perturbation theory, and we have to replace $I^n \rightarrow [l] I_l^n$ in the ‘‘connected’’ terms of perturbation expansion in comparison with the ‘‘standard’’ $s-d$ model ($l=0$).

It is worthwhile to remember the main results for the one-impurity version of this model.^{21,22} Perturbation theory treatment leads to occurrence of infrared divergences. Provided that $I < 0$, the characteristic energy scale (the Kondo temperature) occurs,

$$T_K = D \exp(1/2I\rho), \quad (6)$$

where D is of order of the bandwidth, ρ is the bare density of electron states at the Fermi level with one spin projection. At $T \sim T_K$ the effective $s-f$ interaction becomes very large and the system enters the strong-coupling regime. The electron energy spectrum in this region is determined by the presence of the Abrikosov-Suhl resonance of the width T_K . The properties of the ground state and character of the low-temperature behavior depend crucially on the parameters S and $[l]$. At $2S = [l]$ the Fermi-liquid singlet state occurs. At $2S > [l]$ the localized moment and logarithmic behavior of electronic characteristics retain, but the replacement $S \rightarrow S - [l]/2$ takes place. At $2S < [l]$ a very interesting ‘‘overcompensated’’ regime occurs. Recently the particular case of this regime with $S = 1/2$, $[l] = 2$ (the two-channel Kondo model describing the non-Fermi-liquid behavior, see, e.g., Refs. 17,19,18) has become a subject of great interest.

In the case of the periodic model, the presence or absence of the strong-coupling regime depends also on the character of intersite spin-spin interactions which are described by H_f . This factor will be analyzed in detail below.

The $s-d(f)$ model does not take into account scattering by orbital degrees of freedom.^{24,25,21,26} Another important model, which is used frequently to describe the Kondo effect, is the Coqblin-Schrieffer model. For its periodic version with the $f-f$ exchange interaction of the $SU(N)$ form we have

$$H_f = \frac{1}{2} \sum_{\mathbf{q}} J_{\mathbf{q}} \sum_{M, M' = -S}^S X_{-\mathbf{q}}^{MM'} X_{\mathbf{q}}^{M'M}, \quad (7)$$

$$H_{sf} = -I \sum_{\mathbf{k}\mathbf{k}'MM'} X_{\mathbf{k}'-\mathbf{k}}^{MM'} c_{\mathbf{k}'M'}^\dagger c_{\mathbf{k}M},$$

where $X_{\mathbf{q}}^{MM'}$ are the Fourier transforms of the Hubbard's operators for the localized spin system,

$$X_i^{MM'} = |iM\rangle \langle iM'|$$

$S = (N-1)/2$ is the total angular momentum (this notation is used for the sake of convenience and has a somewhat different meaning in comparison with spin S in the $s-f$ model), and the operators

$$c_{\mathbf{k}M} = \sum_{m\sigma} C_{1/2\sigma,lm}^{SM} c_{\mathbf{k}m\sigma} \quad (8)$$

possess, after averaging over the angles, the Fermi properties due to the orthogonality relations for the Clebsh-Gordan coefficients C . As well as for model (2), we will assume that this averaging should be performed when calculating the Green's functions. The Hamiltonian H_{sf} with $I < 0$ can be derived from the degenerate Anderson-lattice model for rare-earth compounds (LS coupling); a Hamiltonian of the same form occurs in the case of jj coupling (actinide systems).²⁶

For $S = 1/2$, $N = 2$, $l = 0$, models (2) and (7) reduce to the standard $s-f$ model with $S = 1/2$ and coincide. The ground state in the one-impurity Coqblin-Schrieffer model is similar to that in the $s-f$ model with $2S = [l]$, i.e., a complete screening of the localized moment and a Fermi-liquid picture take place. Due to another structure of perturbation theory for the Coqblin-Schrieffer model, we have to replace $2 \rightarrow N$ in Eq. (6). Thus the role of the degeneracy factors in both the models under consideration is different: the expression for T_K does not contain the factor of $[l] = (2l+1)$ in model (2), but contains the factor of N in model (7). Peculiarities of the Coqblin-Schrieffer model are determined by that the transitions between any values of localized f -state projection M are possible, so that the number of excitation branches is large. We shall see that this may result in essential modifications of magnetic behavior. The ground state and the spectrum of magnetic excitations in model (7) are discussed in Appendix A. It is interesting that for an antiferromagnet (AFM) the situation depends on the sign of the next-nearest-neighbor $f-f$ interaction (AFM1 and AFM2 cases).

The interaction H_f in Eq. (7) can be obtained as an indirect RKKY-type interaction which arises in the second order in H_{sf} . Using the standard Heisenberg interaction [as in Eq. (2)], where only $M \rightarrow M \pm 1$ transitions are allowed, is inconvenient since other transitions acquire an energy gap. However, inclusion of this interaction does not lead to a strong change of the physical picture. The standard angular momentum operators on a site are expressed in terms of the X operators as

$$S_i^+ = \sum_M (S-M)^{1/2} (S+M+1)^{1/2} X_i^{M+1,M}, \quad (9)$$

$$S_i^z = \sum_M M X_i^{MM}.$$

Of course, both the $s-f$ exchange model and Coqblin-Schrieffer model are some idealizations of the realistic situation. The choice of an adequate model for a given compound depends mainly on the relation between the width of the f level and the spin-orbital coupling parameter. Provided that the broadening of the f level due to either the hybridization or direct $f-f$ overlap is larger than its spin-orbital splitting we should consider the latter splitting after the transition from the atomiclike f states to crystal states. Usually the orbital momentum is quenched in the Bloch-like states,²⁷ and therefore only the spin momentum should be taken into account when considering the interaction with conduction electrons. The Coqblin-Schrieffer model was initially proposed to describe cerium and ytterbium systems, especially diluted ones.²³ However, as it is clear now, the situation for cerium compounds is more complicated. First, the spin-orbital coupling for cerium is in fact not too large (about 0.25 eV) and comparable with the width of the virtual f level. Second, a number of cerium system, including the pure α -cerium, have rather large $f-f$ overlap (the relative role of $f-f$ overlap and hybridization is discussed in detail in the review²⁸). Thus the applicability of these models should be considered separately for any specific compound. We shall demonstrate below that results of the scaling consideration for the Coqblin-Schrieffer model and $s-f$ exchange models are essentially different.

Model (7) can be generalized to include two magnetic f configurations with the angular momenta J and J' so that

$$H_{sf} = -I \sum C_{J'\mu,jm}^{JM} C_{J'\mu,jm'}^{J'M'} X_{\mathbf{k}'-\mathbf{k}}^{MM'} c_{\mathbf{k}'m'}^\dagger c_{\mathbf{k}m} \quad (10)$$

(we restrict ourselves for simplicity to the case of jj coupling bearing in mind uranium compounds). However, this Hamiltonian has a complicated tensor structure^{21,26} and does not enable one to calculate a unique energy scale by using perturbation expansion. Such an energy scale can be obtained starting from the low-temperature regime and reads²⁶

$$T_K = D \exp \left[-1 / I \rho \left(\frac{2J+1}{2J'+1} - 1 \right) \right] \quad (11)$$

[note that the exponent in Eq. (11) for the case $J' = 0$ differs by a unity from the correct result; such a difference is typical for the methods which are in fact based on the large- N expansion^{29,30}]. In the case $J > J'$ the situation for model (11) is similar to that for the $s-f$ model with $2S > [l]$.

III. SCALING EQUATIONS

Using the perturbation theory results for the renormalizations of the effective $s-f$ parameter and spin-fluctuation energy (Appendixes B–D) we write down the system of scaling equations in the case of the Kondo lattice for various magnetic phases.

We apply the ‘‘poor man scaling’’ approach.³¹ The Kondo effect is connected with the contributions of ‘‘soft’’ electron-hole excitations with the energy $E \rightarrow 0$, which result in infrared divergences. We start from the conduction band which is filled in the energy interval $(-D, 0)$ (here and hereafter the energy is calculated from the Fermi energy $E_F = 0$). It is assumed in the scaling (renormalization-group) ap-

proach that for describing the phenomena related to the soft excitations we can carry out the ‘‘decimation’’ procedure, i.e., excluding high-energy degrees of freedom. Namely, we may describe the occupied electron states with $0 > E > C$ by essentially the same Hamiltonian as the bare one, but with the parameters that are renormalized by virtual transitions from the states in the region $C > E > D$. To perform explicitly the renormalization we can divide this ‘‘hard’’ region in thin layers with the widths δC and calculate the contribution from each layer within perturbation theory subsequently replacing the bare model parameters with the effective ones. To derive the total effect of renormalizations in the effective-Hamiltonian parameters we have to integrate the obtained equations in δC from $-D$ to the flow cutoff parameter C . The fixed point determining the ground state corresponds to $C = 0$.

Thus we have to consider the dependence of the effective (renormalized) s - f exchange parameter on the variable C which occurs at picking out the Kondo singular terms. The detailed consideration will be performed for a ferromagnet in the nondegenerate s - f model (or, equivalently, in the Coqblin-Schrieffer model with $N=2$). To transform the expression for I_{ef} [Eq. (C1)] we calculate the contribution of the intermediate electron states near the Fermi level with $C < t_{\mathbf{k}+\mathbf{q}} < C + \delta C$ in the sums in Eq. (C2). We have

$$\delta I_{ef}(C) = I^2 \sum_{C < t_{\mathbf{k}'} < C + \delta C} \left(\frac{1}{t_{\mathbf{k}'} + \omega_{\mathbf{k}'-\mathbf{k}}} + \frac{1}{t_{\mathbf{k}'} - \omega_{\mathbf{k}'-\mathbf{k}}} \right). \quad (12)$$

Averaging over the Fermi surface $t_{\mathbf{k}} = 0$ we obtain

$$\delta I_{ef}(C) / \delta C = \rho^{-1} I^2 \sum_{\mathbf{k}, \mathbf{k}'} \delta(t_{\mathbf{k}}) \delta(t_{\mathbf{k}'}) \left(\frac{1}{C + \omega_{\mathbf{k}'-\mathbf{k}}} + \frac{1}{C - \omega_{\mathbf{k}'-\mathbf{k}}} \right). \quad (13)$$

We have replaced in Eq. (13) the integration over the surface $t_{\mathbf{k}'} = C$ by that over the surface $t_{\mathbf{k}'} = 0$ since the most important (for picking out the singular contributions) region is $|C| \sim \bar{\omega}$, $\bar{\omega}$ being a characteristic magnon frequency, and therefore $|C| \ll D$. Thus we have to retain the variable C in all the expressions where C is compared to $\bar{\omega}$, and neglect it in the case of comparison with characteristic band energies. The integration in Eq. (13) can be performed explicitly for the simplest ‘‘Debye’’ approximation where the long-wave dispersion law is assumed to hold in the whole Brillouin zone, $\omega_{\mathbf{q}} = D_s q^2$, and a spherical Fermi surface to derive

$$\delta I_{ef}(C) = \frac{\rho I^2}{\bar{\omega}} \delta C \ln \left| \frac{C - \bar{\omega}}{C + \bar{\omega}} \right| \quad (14)$$

with $\bar{\omega} = 4D_s k_F^2$.

To carry out a self-consistent treatment we need the scaling equation for the magnon frequency of the ferromagnet (FM). The singular correction comes from the product of the

Fermi functions in the function Φ^{FM} [see Eq. (D15)]. Picking out in Eq. (D15) the contribution from the electron-hole excitations with the energy in the interval $(C, C + \delta C)$ we obtain

$$\delta \omega_{\mathbf{q}}(C) = -2I^2 S \sum_{\mathbf{k}, \mathbf{k}', C < t_{\mathbf{k}} - t_{\mathbf{k}'} < C + \delta C} (J_{\mathbf{k}'-\mathbf{k}} + J_{\mathbf{q}} - J_{\mathbf{q}+\mathbf{k}-\mathbf{k}'} - J_0) \frac{1}{(t_{\mathbf{k}} - t_{\mathbf{k}'} - \omega_{\mathbf{k}'-\mathbf{k}})^2} \quad (15)$$

To provide the conservation of the number of particles at electron-hole transitions, the integration region in Eq. (15) should be divided symmetrically for electron and holes, namely, either $C/2 < t_{\mathbf{k}} < C/2 + \delta C/2$, $t_{\mathbf{k}'} = -C/2$, or $-C/2 < t_{\mathbf{k}'} < -C/2 + \delta C/2$, $t_{\mathbf{k}} = C/2$. Similar to Eq. (13) we can pass, with the accuracy of C/D , from the averaging over the surface $t_{\mathbf{k}} = \pm C/2$ to that over the Fermi surface. Then we have

$$\delta \omega_{\mathbf{q}}(C) / \delta C = 2I^2 S \sum_{\mathbf{k}, \mathbf{k}'} \delta(t_{\mathbf{k}}) \delta(t_{\mathbf{k}'}) (J_{\mathbf{k}'-\mathbf{k}} + J_{\mathbf{q}} - J_{\mathbf{q}+\mathbf{k}-\mathbf{k}'} - J_0) \left(\frac{1}{C + \omega_{\mathbf{k}'-\mathbf{k}}} + \frac{1}{C - \omega_{\mathbf{k}'-\mathbf{k}}} \right). \quad (16)$$

After passing into the real space, $J_{\mathbf{p}} = \sum_{\mathbf{R}} J_{\mathbf{R}} \exp(i\mathbf{p}\mathbf{R})$, we have to replace

$$\begin{aligned} J_{\mathbf{k}'-\mathbf{k}} &\rightarrow \langle J_{\mathbf{k}'-\mathbf{k}} \rangle_{t_{\mathbf{k}}=t_{\mathbf{k}'}=E_F} \\ &\equiv \rho^{-2} \sum_{\mathbf{k}, \mathbf{k}'} \delta(t_{\mathbf{k}}) \delta(t_{\mathbf{k}'}) J_{\mathbf{k}'-\mathbf{k}} \\ &= \sum_{\mathbf{R}} J_{\mathbf{R}} |\langle e^{i\mathbf{k}\mathbf{R}} \rangle_{t_{\mathbf{k}}=E_F}|^2 \end{aligned} \quad (17)$$

and perform similar transformations in other terms. We obtain

$$\delta \omega_{\mathbf{q}}(C) / \delta C = 2\omega_{\mathbf{q}}(1 - \alpha_{\mathbf{q}}) I^2 \sum_{\mathbf{k}, \mathbf{k}'} \delta(t_{\mathbf{k}}) \delta(t_{\mathbf{k}'}) \left(\frac{1}{C + \omega_{\mathbf{k}'-\mathbf{k}}} + \frac{1}{C - \omega_{\mathbf{k}'-\mathbf{k}}} \right) \quad (18)$$

with

$$\alpha_{\mathbf{q}} = \sum_{\mathbf{R}} J_{\mathbf{R}} |\langle e^{i\mathbf{k}\mathbf{R}} \rangle_{t_{\mathbf{k}}=E_F}|^2 [1 - \cos \mathbf{q}\mathbf{R}] / \sum_{\mathbf{R}} J_{\mathbf{R}} [1 - \cos \mathbf{q}\mathbf{R}]. \quad (19)$$

In the approximation of nearest neighbors at distance d , the quantity α does not depend on \mathbf{q} . For a spherical Fermi surface we have

$$\alpha_{\mathbf{q}} = \alpha = |\langle e^{i\mathbf{k}\mathbf{R}} \rangle_{t_{\mathbf{k}}=E_F}|^2 = \left(\frac{\sin k_F d}{k_F d} \right)^2. \quad (20)$$

Hereafter we set $\alpha = \text{const}$. Then we may use in further consideration of the scaling equations a single renormalization

parameter, rather than the whole function of \mathbf{q} . In the ‘‘Debye’’ approximation for the spherical Fermi surface we obtain

$$\delta \bar{\omega}_{ef}(C) = 2\rho^2 I^2 (1 - \alpha) \delta C \ln \left| \frac{C - \bar{\omega}}{C + \bar{\omega}} \right|. \quad (21)$$

The ‘‘Kondo’’ correction to magnetization occurs from the same magnon Green’s function [see Eq. (D11)], so that we derive

$$\delta \bar{S}_{ef}(C) = \frac{\rho^2 I^2 S}{\bar{\omega}} \delta C \ln \left| \frac{C - \bar{\omega}}{C + \bar{\omega}} \right|. \quad (22)$$

We see that the same functional dependence occurs in Eqs. (14), (21), and (22). This property turns out to take place in all the cases under consideration.

The treatment of other magnetic phases, as well as of more complicated models, is performed in a similar way. Using Eqs. (B5), (C2), (C5) we obtain for model (2), and for the paramagnetic (PM), FM, and AFM2 phases in the Coqblin-Schrieffer model the renormalizations of effective coupling in the form

$$\delta I_{ef}(C) = N\rho I^2 \eta \left(-\frac{\bar{\omega}}{C} \right) \delta C/C, \quad (23)$$

where $\bar{\omega}$ is a characteristic spin-fluctuation energy, $N=2$ for the $s-f$ model, $\eta(x)$ is the scaling function which satisfies the condition $\eta(0)=1$ (this guarantees the correct one-impurity limit treated in Ref. 31). Taking into account the results of Appendix B we obtain for the paramagnetic phase

$$\eta^{\text{PM}} \left(\frac{\bar{\omega}}{C} \right) = \text{Re} \int_{-\infty}^{\infty} d\omega \langle \mathcal{J}_{\mathbf{k}-\mathbf{k}'}(\omega) \rangle_{t_{\mathbf{k}}=t_{\mathbf{k}'}=E_F} \times \frac{1}{1 - (\omega + i0)^2/C^2}. \quad (24)$$

For the FM and AFM phases we have

$$\eta^{\text{FM}} \left(\frac{\bar{\omega}}{C} \right) \equiv \frac{1}{N} \left[(N-1) \eta_{\uparrow} \left(\frac{\bar{\omega}}{C} \right) + \eta_{\downarrow} \left(\frac{\bar{\omega}}{C} \right) \right], \quad (25)$$

$$\eta_{\uparrow, \downarrow}^{\text{FM}} \left(-\frac{\bar{\omega}}{C} \right) = \langle (1 \mp \omega_{\mathbf{k}-\mathbf{k}'}/C)^{-1} \rangle_{t_{\mathbf{k}}=t_{\mathbf{k}'}=E_F},$$

$$\eta^{\text{AFM}} \left(-\frac{\bar{\omega}}{C} \right) = \langle (1 - \omega_{\mathbf{k}-\mathbf{k}'}/C^2)^{-1} \rangle_{t_{\mathbf{k}}=t_{\mathbf{k}'}=E_F}. \quad (26)$$

Using the spin-diffusion approximation Eq. (B6) in Eq. (24) and the approximations $\omega_{\mathbf{q}}^{\text{FM}} = D_s q^2$, $\omega_{\mathbf{q}}^{\text{AFM}} = c_s q$ (which are justified, e.g., at small k_F), we get $\bar{\omega} = 4\mathcal{D}k_F^2$ for a paramagnet, $\bar{\omega} = \omega_{2k_F}$ for the FM and AFM cases,

$$\eta^{\text{PM}}(x) = x^{-1} \arctan x,$$

$$\eta_{\uparrow, \downarrow}^{\text{FM}}(x) = \pm x^{-1} \ln |1 \pm x|, \quad (27)$$

$$\eta^{\text{AFM}}(x) = \begin{cases} -x^{-2} \ln |1 - x^2|, & d=3 \\ (1 - x^2)^{-1/2} \theta(1 - x^2), & d=2, \end{cases}$$

where $\theta(x)$ is the step function, $d=3$ for PM and FM.

One can see that the scaling functions (27) for the ordered phases contain singularities at $x=1$. It may be demonstrated by direct calculations according to Eqs. (25), (26) that the presence of such a singularity is a general property which does not depend on the model assumptions about the form of electron and magnon spectra. In the general case, the singularity occurs at $C = -\omega_{\mathbf{q}_m}$ where \mathbf{q}_m corresponds to the maximum diameter of the Fermi surface.

The functions $\eta_{\uparrow}^{\text{FM}}(x)$ and $\eta^{\text{AFM}}(x)$ ($d=3$) change their sign at $x=2$ and $x=\sqrt{2}$, respectively. For $d=2$ the function $\eta^{\text{AFM}}(x)$ vanishes discontinuously at $x>1$, but a smooth contribution occurs for more realistic models of magnon spectrum.

When considering characteristics of the localized-spin subsystem, the lowest-order Kondo corrections originate from double integrals over both electron and hole states [see Eqs. (B9), (D10), (D6)]. Then we have to introduce two flow parameters C_e and C_h with $C_e + C_h = C$ (C is the flow parameter for the electron-hole excitations). In the FM case for the Coqblin-Schrieffer model we have $\delta C_h = -(N-1)\delta C_e$ due to the requirement of the number-of-particle conservation in electron-hole transitions (there exists $N-1$ ‘‘channels’’ for electrons and one ‘‘channel’’ for holes). For PM and AFM2 cases in the Coqblin-Schrieffer model, as well as for all the cases in the $s-f$ model, the electron-hole symmetry is not violated and we have $\delta C_e = -\delta C_h$.

Taking into account Eqs. (B9), (D20), (D26) we obtain

$$\delta \bar{S}_{ef}(C)/S = V\rho \delta I_{ef}(C) = VN\rho^2 I^2 \eta \left(-\frac{\bar{\omega}}{C} \right) \delta C/C, \quad (28)$$

where $V=[I]$ for the $s-f$ model, $V=1$ for the PM and FM phases in the Coqblin-Schrieffer model, and $V=2/N$ for the AFM2 phase. The renormalizations of spin-wave frequencies are obtained in a similar way from Eqs. (B13), (D14), (D13), (D20), (D27), and are given by

$$\delta \bar{\omega}_{ef}(C)/\bar{\omega} = a \delta \bar{S}_{ef}(C)/S = aVN\rho^2 I^2 \eta \left(-\frac{\bar{\omega}}{C} \right) \delta C/C, \quad (29)$$

where, in the nearest-neighbor approximation,

$$a = \begin{cases} 1 - \alpha & \text{PM} \\ 2(1 - \alpha) & \text{FM} \\ 1 & \text{AFM.} \end{cases} \quad (30)$$

Introducing the dimensionless coupling constants

$$g_{ef}(C) = -N\rho I_{ef}(C), \quad g = -N\rho I$$

and replacing in the right-hand sides of Eqs. (23), (29), (28) $g \rightarrow g_{ef}(C)$, $\bar{\omega} \rightarrow \bar{\omega}_{ef}(C)$, we obtain the system of scaling equations

$$\partial g_{ef}(C)/\partial C = -\Lambda, \quad (31)$$

$$\partial \ln \bar{\omega}_{ef}(C) / \partial C = aV\Lambda / N, \quad (32)$$

$$\partial \ln \bar{S}_{ef}(C) / \partial C = V\Lambda / N, \quad (33)$$

with

$$\Lambda = \Lambda(C, \bar{\omega}_{ef}(C)) = [g_{ef}^2(C)/C] \eta(-\bar{\omega}_{ef}(C)/C). \quad (34)$$

As regards the AFM1 state in the Coqblin-Schrieffer model (Appendix A), its treatment in a general case is a difficult and cumbersome problem. However, one can see from Eq. (D24) that to leading approximation in $1/N$ the scaling equations coincide with those for the FM state with the replacement $J_p \rightarrow J_p^{(2)}$.

IV. IMPROVED VERSION OF SCALING EQUATIONS: AN ACCOUNT OF DISSIPATIVE CONTRIBUTIONS TO SPIN DYNAMICS IN THE ORDERED PHASES

As follows from the results of the previous section, passing from the dissipative spin dynamics, which is characteristic for the PM phase, to the dynamics with well-defined spin-wave excitations (ordered FM and AFM phases) results in the occurrence of singularities in the scaling function $\eta(x)$ at $x \rightarrow 1$. It will be shown below that this leads to a decrease of the critical value of the coupling constant g_c . One may suppose that in the situation of strongly suppressed saturation moment (g is close to g_c) the character of spin dynamics in the ordered phases should change drastically. By the analogy with weak itinerant magnets³² one may expect that for $\bar{S} \ll S$ a considerable part of the localized-spin spectral density comes from the branch cut of the spin Green's function rather than from the magnon pole.

In this section we shall demonstrate that this indeed takes place provided that our approach is slightly modified. To this end we shall analyze the structure of the spin Green's function with account of the singular Kondo corrections in more detail.

First we consider the case of a ferromagnet within the $s-f$ model. We have near the magnon pole

$$\langle \langle S_{\mathbf{q}}^+ | S_{-\mathbf{q}}^- \rangle \rangle_{\omega} = \frac{2\bar{S}Z_{\mathbf{q}}}{\omega - \omega_{\mathbf{q}}^{ef}} + \langle \langle S_{\mathbf{q}}^+ | S_{-\mathbf{q}}^- \rangle \rangle_{\omega}^{\text{incoh}}, \quad (35)$$

where the residue at the pole is determined by Eq. (D14):

$$1/Z_{\mathbf{q}} - 1 = - \left(\frac{\partial \omega_{\mathbf{q}}(\omega)}{\partial \omega} \right)_{\omega=\omega_{\mathbf{q}}} \simeq - [I] \sum_{\mathbf{p}} \Phi_{\mathbf{p}00}^{\text{FM}}. \quad (36)$$

Besides that, there exists the singular contribution which comes from the incoherent (nonpole) part of the spin spectral density. To calculate the renormalization of g we use, instead of Eq. (C2), the representation of the electron self-energy in terms of the spectral density (see the detailed derivation in Ref. 9)

$$\Sigma_{\mathbf{k}\uparrow}^{\text{FM}}(E) = -\frac{1}{\pi} R I^2 \int_{-\infty}^{\infty} d\omega \sum_{\mathbf{q}} \frac{n_{\mathbf{k}-\mathbf{q}}}{E - t_{\mathbf{k}-\mathbf{q}} + \omega} \text{Im} \langle \langle S_{\mathbf{q}}^+ | S_{-\mathbf{q}}^- \rangle \rangle_{\omega},$$

$$\Sigma_{\mathbf{k}\downarrow}^{\text{FM}}(E) = -\frac{1}{\pi} R I^2 \int_{-\infty}^{\infty} d\omega \sum_{\mathbf{q}} \frac{1 - n_{\mathbf{k}-\mathbf{q}}}{E - t_{\mathbf{k}-\mathbf{q}} - \omega} \text{Im} \langle \langle S_{\mathbf{q}}^+ | S_{-\mathbf{q}}^- \rangle \rangle_{\omega}. \quad (37)$$

Thus the magnon pole contribution to g_{ef} is multiplied by Z , and the incoherent one by $1 - Z$. The renormalizations of $\bar{\omega}_{ef}$ and Z are obtained in the same way as in the previous section. We derive in the nearest-neighbor approximation

$$\partial g_{ef}(C) / \partial C = -\Lambda, \quad (38)$$

$$\partial \ln \bar{\omega}_{ef}(C) / \partial C = aV\Lambda / N, \quad (39)$$

$$\partial (1/Z) / \partial C = \partial \ln \bar{S}_{ef}(C) / \partial C = V\Lambda / N, \quad (40)$$

where $a = 2(1 - \alpha)$, $N = 2$

$$\Lambda = [g_{ef}^2(C)/C] [Z \eta_{\text{coh}}(-\bar{\omega}_{ef}(C)/C) + (1 - Z) \eta_{\text{incoh}}(-\bar{\omega}_{ef}(C)/C)], \quad (41)$$

$\eta_{\text{coh}} = \eta^{\text{FM}}$, and the function η_{incoh} is, generally speaking, unknown. For further estimations we put below $\eta_{\text{incoh}} = \eta^{\text{PM}}$. Apparently, this overestimates the role of incoherent contributions (the true spin dynamics in the paramagnetic phase should take into account short-range order). However, such an approximation enables us to investigate the sensitivity of various physical properties to the inclusion of η_{incoh} .

The account of the incoherent part does not modify strongly numerical results (see Sec. VI). At the same time, the physical picture of magnetism changes considerably. According to Eq. (40) we have

$$\frac{1}{Z(\xi)} = 1 + \ln \frac{S}{\bar{S}(\xi)}. \quad (42)$$

Consequently, the increase of magnetic moment owing to the Kondo screening leads to a suppression of magnon contributions to the spectral density. Unlike the case of weak itinerant magnets, this suppression is logarithmic in the ground-state magnetization.

In the case of an antiferromagnet the calculations are performed by taking into account expressions (D2), (D3). In the nearest-neighbor approximation ($J_{\mathbf{Q}+\mathbf{q}} = -J_{\mathbf{q}}$) we obtain

$$\langle \langle S_{\mathbf{q}}^+ + S_{\mathbf{q}}^- | S_{-\mathbf{q}}^+ + S_{-\mathbf{q}}^- \rangle \rangle_{\omega}^{\text{coh}} \simeq \frac{8S^2(J_0 - J_{\mathbf{q}})}{\omega^2 - (\omega_{\mathbf{q}}^{ef})^2} \left(1 - [I] \sum_{\mathbf{p}} \Phi_{\mathbf{p}00}^{\text{AFM}} \right) \quad (43)$$

[the quantity (43) just determines the Kondo renormalization of electron spectrum, cf. Ref. 13]. Then the scaling equations for the AFM differ from those for the FM by the replacement $a \rightarrow 1$ in Eqs. (38)–(40) only.

V. THE SCALING BEHAVIOR IN THE LARGE- N COQBLIN-SCHRIEFFER MODEL

It is instructive to consider the limit $N \rightarrow \infty$ (to avoid misunderstanding, it should be noted that this limit with inclu-

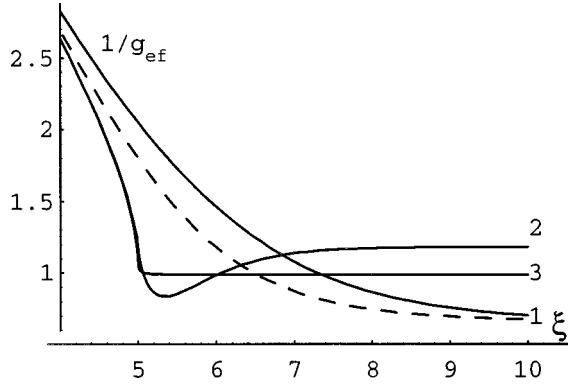


FIG. 1. The dependence $1/g_{ef}$ on $\xi = \ln|D/C|$ in the large- N limit with $\lambda = \ln(D/\bar{\omega}) = 5$, $g = 0.15$ for a paramagnet (dashed line) and different magnetic phases (solid lines): (1) ferromagnet (2) 3D antiferromagnet (3) 2D antiferromagnet.

sion of spin dynamics in the zeroth approximation differs somewhat from the considerations of Refs. 30 and 29). Then the renormalizations of spin dynamics and \bar{S}_{ef} are absent, and the transition into the nonmagnetic Kondo-lattice state cannot be described. However, peculiarities of the dependence $g_{ef}(C)$ for various types of magnetic ordering are described qualitatively, explicit analytical expressions being obtained. We have

$$1/g_{ef}(C) - 1/g = G(C) = - \int_{-D}^C \frac{dC'}{C'} \eta \left(-\frac{\bar{\omega}}{C'} \right), \quad (44)$$

where D is the cutoff energy defined by $g_{ef}(-D) = g$ (see Sec. III). Performing the integration we obtain

$$G^{\text{PM}}(C) = \frac{1}{2} \ln[(C^2 + \bar{\omega}^2)/D^2] + \frac{C}{\bar{\omega}} \arctan\left(\frac{\bar{\omega}}{C}\right) - 1, \quad (45)$$

$$G^{\text{FM}}(C) = \ln|C/D| - (C/\bar{\omega} - 1) \ln|1 - \bar{\omega}/C| + 1, \quad (46)$$

$$G^{\text{AFM}}(C) = \ln|C/D| - \frac{1}{2} [(C^2/\bar{\omega}^2 - 1) \ln|1 - \bar{\omega}^2/C^2| - 1], \quad (47)$$

$d=3,$

$$G^{\text{AFM}}(C) = \theta(|C| - \bar{\omega}) \ln \left(\frac{1}{2} (|C| + \sqrt{C^2 - \bar{\omega}^2})/D \right) + \theta(\bar{\omega} - |C|) \ln(\bar{\omega}/2D), \quad d=2. \quad (48)$$

The dependences $1/g_{ef}(\xi = \ln|D/C|)$ are shown in Fig. 1. The effective coupling constant $g_{ef}(C)$ begins to deviate strongly from its one-impurity behavior

$$1/g_{ef}(C) = 1/g - \ln|D/C| \quad (49)$$

at $|C| \sim \bar{\omega}$. One can see that at small $\bar{\omega} \ll |C|$ spin dynamics result in a decrease of $g_{ef}(C)$ for the PM and FM cases, and in an increase for the AFM case.

It should be noted that Eq. (44) can be used even for $N=2$ provided that g is considerably smaller than the critical value g_c (see the next section). Besides that, Eq. (44) works

in the PM and FM phases provided that k_F is small, so that, according to Eq. (20), $\alpha \rightarrow 1$. However, in the case of the ferromagnet we have instead of Eq. (46)

$$G^{\text{FM}}(C) = \ln|C/D| - \frac{N-1}{N} (C/\bar{\omega} - 1) \ln|1 - \bar{\omega}/C| + \frac{1}{N} (C/\bar{\omega} + 1) \ln|1 + \bar{\omega}/C| + 1. \quad (50)$$

In the three-dimensional (3D) AFM case $1/g_{ef}(C)$ has a minimum with decreasing $|C|$. For a 2D AFM, $1/g_{ef}$ has a square-root singularity at $|C| < \bar{\omega}$ and becomes constant at $|C| > \bar{\omega}$. As we shall see in the next section, these features retain at finite N . For a ferromagnet, the singularity is absent at $N \rightarrow \infty$ since only the contribution of η_{\uparrow} survives. However, it is present for finite N due to contribution of η_{\downarrow} . Note that, contrary to the case $N \rightarrow \infty$, for an FM with $N=2$ spin dynamics results in a decrease of $g_{ef}(C)$ at not too small C .

The boundary of the strong-coupling region (the renormalized Kondo temperature) is determined by $G(C = -T_K^*) = -1/g$. Of course, T_K^* means here only some characteristic energy scale extrapolated from high temperatures, and the detailed description of the ground state requires a more advanced consideration. In the PM and FM phases spin dynamics suppresses T_K^* . On the other hand, in the AFM case spin dynamics at not too large $\bar{\omega}$ results in an increase of T_K^* .

Provided that the strong-coupling regime does not occur, i.e., g is smaller than the critical value g_c , $g_{ef}(C \rightarrow 0)$ tends to a finite value g^* . To leading order in $\ln(D/\bar{\omega})$ we have

$$1/g_c = \lambda \equiv \ln(D/\bar{\omega}). \quad (51)$$

However, an account of next-order terms results in an appreciable dependence on the type of magnetic ordering and space dimensionality. For PM, FM, and 2D AFM phases the critical value g_c is given by $1/g_c = -G(0)$. Then we obtain

$$1/g^* = 1/g - 1/g_c \quad (52)$$

with

$$1/g_c = \lambda + \begin{cases} 1, & \text{PM, FM} \\ \ln 2, & \text{2D AFM.} \end{cases} \quad (53)$$

At the same time, in the 3D AFM case g_c is determined by the minimum of the function $G(C)$. Thus g^* remains finite at $g \rightarrow g_c - 0$:

$$1/g^* = 1/g - 1/g_c + 1/g_c^*, \quad (54)$$

where

$$1/g_c = \lambda + (1 + \ln 2)/2, \quad (55)$$

$$1/g_c^* = \Delta = (\ln 2)/2 \approx 0.35$$

Δ being the depth of the minimum.

For $C \rightarrow 0$ we have

$$G(C) - G(0) \approx \begin{cases} \pi|C|/2\bar{\omega} & \text{PM,} \\ |C/\bar{\omega}|\ln|\bar{\omega}/C| & \text{FM,} \\ -(C/\bar{\omega})^2\ln|\bar{\omega}/C| & \text{3D AFM} \end{cases} \quad (56)$$

[however, $G^{\text{FM}}(C) - G^{\text{FM}}(0) \approx (C/\bar{\omega})^2$ for function (50) at $N=2$]. As follows from Eq. (56), for $g \rightarrow g_c + 0$ we have in the PM and FM cases to logarithmic accuracy

$$T_K^* \approx \bar{\omega} \frac{g - g_c}{g_c^2} \times \begin{cases} 2/\pi, & \text{PM} \\ \ln[(g - g_c)/g_c], & \text{FM.} \end{cases} \quad (57)$$

On the other hand, in the AFM phases T_K^* is finite at $g \rightarrow g_c + 0$:

$$T_K^{*c} = \bar{\omega} \times \begin{cases} 1, & \text{2D AFM} \\ 1/\sqrt{2}, & \text{3D AFM.} \end{cases} \quad (58)$$

VI. SCALING BEHAVIOR FOR FINITE N

Some results obtained in the large- N limit hold in the finite- N case too, but there occur here a number of new important features. To consider the general case we write down the first integral of the system Eqs. (31) and (32)

$$g_{ef}(C) + (N/Va)\ln\bar{\omega}_{ef}(C) = \text{const}, \quad (59)$$

which results in

$$\bar{\omega}_{ef}(C) = \bar{\omega} \exp(-(aV/N)[g_{ef}(C) - g]). \quad (60)$$

As follows from Eqs. (32) and (33)

$$\frac{\bar{S}_{ef}(C)}{S} = \left(\frac{\bar{\omega}_{ef}(C)}{\bar{\omega}} \right)^{1/a}. \quad (61)$$

Substituting Eq. (60) into Eq. (31) we obtain

$$\partial(1/g_{ef})/\partial\xi = -\Psi(\lambda + (aV/N)[g_{ef} - g] - \xi), \quad (62)$$

where

$$\Psi(\xi) = \eta(e^{-\xi}), \quad \xi = \ln|D/C|, \quad \lambda = \ln(D/\bar{\omega}) \gg 1.$$

The presence of g_{ef} in the argument of the function Ψ in Eq. (62) leads to drastic changes in the scaling behavior in comparison with the large- N limit. We describe below the renormalization process in various cases.

If g is sufficiently large, the increase of g_{ef} will lead to that the argument of Ψ will never be small, so that the scaling behavior will be essentially the one-impurity one. At smaller g the function $1/g_{ef}(\xi)$ begins to deviate strongly from the one-impurity behavior $1/g_{ef}(\xi) = 1/g - \xi$ starting from $\xi \approx \xi_1$ where ξ_1 is the minimal solution to the equation

$$\lambda + (aV/N)[g_{ef}(\xi) - g] = \xi. \quad (63)$$

If the argument remains negative with further increasing ξ , $1/g_{ef}(\xi)$ will decrease tending to the finite value g^* , the derivative $\partial(1/g_{ef})/\partial\xi$ being exponentially small, so that the situation is close to the large- N case (Fig. 1). However, $(aV/N)g_{ef}(\xi)$ can increase more rapidly than ξ , so that the second solution to Eq. (63), ξ_2 will occur, and the argument

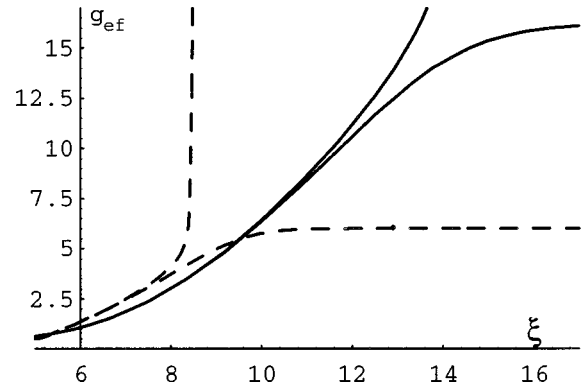


FIG. 2. The scaling trajectories $g_{ef}(\xi)$ in a paramagnet ($g=0.15392 > g_c$, upper solid line, and $g=0.15391 < g_c$, lower solid line) and a ferromagnet ($g=0.13868 > g_c$, upper dashed line, and $g=0.13867 < g_c$, lower dashed line) according to Eq. (62) with $N=2$, $\alpha=1/2$, $\lambda=5$, $\delta=1/100$.

of the function Ψ becomes positive again. Then $g_{ef}(\xi)$ will diverge at some point $\xi^* = \ln|D/T_K^*|$. The divergence is described, unlike the large- N limit, by the law

$$g_{ef}(\xi) \approx 1/(\xi^* - \xi), \quad (64)$$

since $\eta(x \ll 1) = 1$. The behavior (64) takes place starting from $\xi \approx \xi_2$.

The dependences $g_{ef}(\xi)$ in the PM case at small $|g - g_c|$ are shown in Fig. 2. The behavior $g_{ef}(\xi)$ between ξ_1 and ξ_2 is nearly linear, but is somewhat smeared since $\Psi(\xi)$ differs considerably from the asymptotic values 0 and 1 in a rather large interval of ξ .

The case of the magnetically ordered phases has a number of peculiarities. Here the singularity of the function $\Psi(\xi)$ at $\xi=0$ turns out to play a crucial role. In particular, one can prove that g_{ef} diverges at some ξ at arbitrarily small g (i.e., $g_c=0$) unless the singularity cutoff is introduced. Indeed, when approaching the singularity point with increasing ξ , the derivative $\partial g_{ef}/\partial\xi$ rapidly increases, and the argument of the function Ψ in Eq. (62) inevitably starts to increase at some point ξ_1 . Thus the singularity point cannot be crossed, and the argument of the function Ψ is always positive. Since $\Psi(\xi' > 0) > 1$, we have $\partial(1/g_{ef})/\partial\xi < -1$ at arbitrary ξ . Therefore the effective coupling constant diverges at $\xi = \xi^* < 1/g$.

To make the value of g_c finite, one has to cut the singularity of the scaling functions. This may be performed by introducing small imaginary parts, i.e., replacing in Eq. (27)

$$\ln|1-x| \rightarrow \frac{1}{2} \ln[(1-x)^2 + \delta^2], \quad (65)$$

$$(1-x)^{-1/2} \theta(1-x) \rightarrow \text{Re}(1-x+i\delta)^{-1/2}$$

$$= \{[(1-x)^2 + \delta^2]^{1/2} + 1-x\}^{1/2} / [(1-x)^2 + \delta^2]^{1/2}.$$

Then Ψ becomes bounded from above:

$$\Psi_{\max} = \eta_{\max} \approx \eta(1) \approx \begin{cases} \frac{1}{2} \ln \delta, & \text{FM} \\ \ln \delta, & \text{3D AFM} \\ \frac{1}{2} \delta^{-1/2}, & \text{2D AFM.} \end{cases} \quad (66)$$

Another way to cut the divergence in the 2D AFM case is to retain strictly the proportionality to the step function,

$$(1-x)^{-1/2}\theta(1-x) \rightarrow \text{Re}(1-x+i\delta)^{-1/2}\theta(1-x), \quad (67)$$

so that $\Psi(\xi)$ cannot take small values.

The value of δ should be determined by the magnon damping at $q=|\mathbf{k}-\mathbf{k}'| \approx 2k_F$ [see Eqs. (25) and (26)]. This damping is due to both exchange and relativistic interactions. The damping owing to exchange scattering by conduction electrons should be formally neglected within the lowest-order scaling consideration, since this contains a more high power of I . The magnon-magnon interaction in the Heisenberg model gives the damping at nonzero temperatures only. However, the relativistic (e.g., dipole) interactions give a damping at $T=0$ due to zero-point oscillations. Hereafter we put in numerical calculations $\delta=1/100$.

The behavior of the solutions to Eq. (62) in magnetic phases for g which is well below g_c is similar to that in the large- N limit (Sec. V). In particular, the function $1/g_{ef}(\xi)$ has a minimum in the 3D AFM case with the same depth. The presence of the minimum may result in nonmonotonic temperature dependences of the physical quantities which are sensitive to the Kondo screening, e.g., of the effective magnetic moment. These dependences are obtained qualitatively by the replacement $|C| \rightarrow T$ in Eqs. (60) and (61). Of course, the standard monotonic spin-wave corrections should be added to the Kondo contributions.

It is important that, except for a very narrow region near g_c , at approaching g_c the value of g^* becomes practically constant, $g^* \approx g(\xi_1) = g_1$. This value is estimated as

$$(aV/N)(\partial g_{ef}/\partial \xi)_{\max} = (aV/N)g_1^2\Psi_{\max} = 1. \quad (68)$$

On the other hand, we may estimate from the linear asymptotics $1/g_{ef}(\xi) \approx 1/g - \xi$ [which holds up to $\xi \approx \xi_1 \approx \lambda + (aV/N)g_1$]

$$1/g_1 \approx 1/g - \xi_1. \quad (69)$$

Comparing Eqs. (69) and (68) we derive the rough estimation

$$1/g_c = \lambda + (aV/N)g_1 + 1/g_1 = \lambda + (N\Psi_{\max}/aV)^{-1/2} + (aV\Psi_{\max}/N)^{1/2}. \quad (70)$$

The value of $1/g_2$ can be also estimated from the linear asymptotics (64):

$$1/g_2 \approx \xi^* - \xi_2. \quad (71)$$

Owing to the singularity, ξ_2 is close to ξ_1 except for very small $|g - g_c|$. In the latter case the behavior $g(\xi_1 < \xi < \xi_2)$ is practically linear,

$$(aV/N)g_{ef}(\xi_1 < \xi < \xi_2) \approx \xi - \lambda \quad (72)$$

(this behavior is discussed in detail in the next sections). This is explained by that the argument of the function Ψ in Eq. (62) should be nearly zero. The behavior at $\xi > \xi_2$ is described by Eq. (64). We may estimate from Eq. (71)

$$\xi^* \approx 1/g + 1/g_2 - 1/g_1. \quad (73)$$

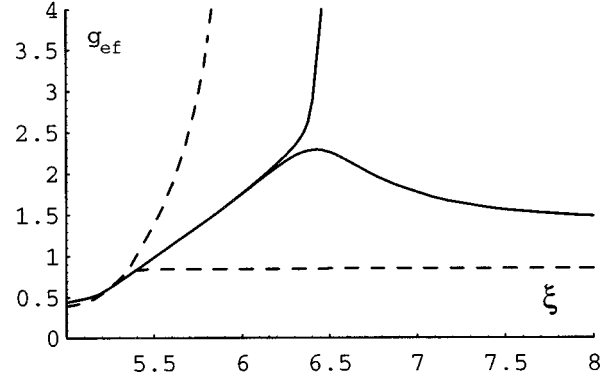


FIG. 3. The scaling trajectories $g_{ef}(\xi)$ in a 3D antiferromagnet (solid lines, $g=0.1320382 > g_c$ and $g=0.1320381 < g_c$) and a 2D antiferromagnet (dashed lines, $g=0.1266714 > g_c$ and $g=0.1266713 < g_c$) according to Eq. (62) with the same parameter values as in Fig. 2.

For the cutoff Eq. (67) with $\eta(x > 1) = 0$ in the 2D AFM case (and in similar situations) ξ^* tends to a finite limit ξ_c^* at $g \rightarrow g_c + 0$. Indeed, as follows from the form of the scaling function (27), one has up to the divergence point $\Psi(\xi) > 1$, so that $\xi^* < 1/g < 1/g_c$. In such a situation g^* turns out to be also finite at $g \rightarrow g_c - 0$, and the character of approaching g_c is quite different from that in the large- N limit. With increasing g , the position of the $1/g_{ef}(\xi)$ singularity point is shifted right due to rapid increase of g_{ef} in the argument of the function Ψ in Eq. (62). The shift should stop at $\xi_1 < \xi_c^*$. This takes place just at $g \rightarrow g_c - 0$. Thus $1/g_{ef}(\xi)$ should vanish discontinuously at $g = g_c$. The ‘‘maximum’’ value of $g_{ef}(\xi)$, $g_{ef}^{\max} = g_c^*$, is estimated from

$$\lambda + (aV/N)(g_{ef}^{\max} - g_c) - \xi_1 = 0. \quad (74)$$

Since for $g > g_c$ the decrease $1/g_{ef}(\xi)$ at $\xi > \xi_1$ is practically linear [see Eq. (64)], we may estimate

$$\xi_c^* - \xi_1 \approx 1/g_{ef}^{\max}. \quad (75)$$

If we accept the cutoff Eq. (65), a small increase of ξ^* and $1/g^*$ will take place in an extremely narrow region near g_c . This increase cannot be practically observed.

In the 3D AFM case the statement about the finiteness of ξ_c^* does not, strictly speaking, hold since there exists a small region where $\Psi(\xi)$ is positive and takes arbitrarily small positive values, so that the decrease of $1/g_{ef}(\xi)$ can be slow. However, the behavior $\xi^*(g)$ is in fact determined by the logarithmic singularity of the function $\Psi(\xi)$ except for a very narrow region near g_c . The numerical calculations yield the estimation $g - g_c \sim 10^{-4}$ for the region where ξ^* starts to increase. Thus, from the practical point of view, we may put ξ_c^* to be finite. The corresponding value of $g_c^{\max} = g_1$ is determined by Eq. (74) and g_1^* is smaller than g_{ef}^{\max} . At very small $g - g_c \sim 10^{-4}$ the value of g^* starts to increase. However, due to the minimum of the function $1/g_{ef}(\xi)$, $g_c^* = 1/\Delta$ remains finite at $g \rightarrow g_c$, as well as in the limit $N \rightarrow \infty$.

In the case of a ferromagnet the influence of the singularity is somewhat weaker since $\Psi(\xi)$ does not change its sign

and takes small positive values up to infinity, so that ξ^* starts to increase appreciably at $g - g_c \sim 10^{-3}$.

The dependences $g_{ef}(\xi)$ according to Eq. (62) for the magnetically ordered phases at $g \rightarrow g_c \pm 0$ are shown in Figs. 2 and 3. One can see that considerable linear regions occur in these dependences for the FM and 3D AFM states.

Now we discuss the results of the approach of Sec. IV, which takes into account the incoherent part of the spin spec-

tral density. The integral of motion of the system of equations (38) and (39) has the same form (59), and we obtain

$$\frac{1}{Z(\xi)} = 1 + \frac{1}{a} \ln \frac{\bar{\omega}}{\omega_{ef}(\xi)} = 1 + \frac{V}{N} [g_{ef}(\xi) - g]. \quad (76)$$

The corresponding equation for g_{ef} reads

$$\frac{\partial(1/g_{ef})}{\partial \xi} = -\Psi_{\text{incoh}}(\lambda + (aV/N)[g_{ef} - g] - \xi) - [\Psi_{\text{coh}}(\lambda + (aV/N)[g_{ef} - g] - \xi) - \Psi_{\text{incoh}}(\lambda + (aV/N)[g_{ef} - g] - \xi)] / \left[1 + \frac{V}{N}(g_{ef} - g) \right]. \quad (77)$$

The role of the incoherent contribution becomes important only provided that Z deviates appreciably from unity, i.e., $g_{ef} - g$ is large. This takes place in a rather narrow region of $|g - g_c|$. The estimation for g_1 in the case of small δ now reads

$$\frac{aVg_1^2/N}{1 + Vg_1/N} \Psi_{\text{coh}}^{\text{max}} = 1, \quad (78)$$

so that, as follows from Eq. (70), g_c increases.

The dependences $g_{ef}(\xi)$ for a ferromagnet at small $|g - g_c|$ according to Eq. (77) are shown in Fig. 4. One can see that the well-linear ‘‘ferromagnetic’’ behavior crosses over to a PM-like ‘‘quasilinear’’ behavior with increasing ξ , cf. Fig. 2. The point of the crossover is estimated from $Z\Psi_{\text{coh}}^{\text{max}} \approx 1$, i.e.,

$$(V/N)(\xi - \lambda) \approx \Psi_{\text{coh}}^{\text{max}}. \quad (79)$$

As demonstrated by numerical calculations, taking account of the incoherent contribution results in smearing of the nonmonotonous behavior of $g_{ef}(\xi)$ in the 3D AFM case,

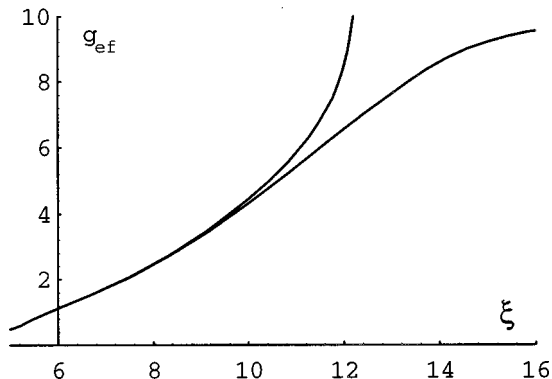


FIG. 4. The scaling trajectories $g_{ef}(\xi)$ in a ferromagnet with account of the incoherent contribution according to Eq. (77) with $N=2$, $\alpha=1/2$, $\lambda=5$, $\delta=1/100$ for $g=0.13997 > g_c$ (upper line) and $g=0.13996 < g_c$ (lower line).

and in some region of $|g - g_c|$ the minimum of $1/g_{ef}(\xi)$ vanishes completely. Therefore $g^* \rightarrow 0$ at $g \rightarrow g_c$, unlike the situation for Eq. (62).

The influence of the incoherent contribution on ξ^* and g^* is considerably suppressed by the singularity of the function $\Psi_{\text{coh}}(\xi)$. The region where this contribution starts to play a role is determined by the quantity δ . In particular, for the 2D AFM case its influence on ξ^* is practically absent since the divergence of $g_{ef}(\xi)$ occurs due to the singularity of $\Psi_{\text{coh}}(\xi)$. Note that since g^* is finite at $g \rightarrow g_c$, the coherent contribution survives up to g_c .

The comparison of the results of various approximations is presented in Table I. One can see from this table that for $N=2$ the relation of the g_c values in the ordered phases and in the PM case is reversed in comparison with the limit $N \rightarrow \infty$. This fact is due to the influence of the scaling function singularities. It should be noted that at larger $\delta \sim 1/5$ the value of g_c in the ordered phases exceeds g_c^{PM} , as well as in the large- N case. In case (ii) the value of g_c is intermediate between $g_c^{(i)}$ and g_c^{PM} and closer to $g_c^{(i)}$. With increasing α or N the difference between $g_c^{(ii)}$ and $g_c^{(i)}$ becomes still smaller.

The dependences $1/g^*(g)$ and $\xi^*(g)$ according to Eq. (77) are shown in Fig. 5 (of course, these diagrams do not

TABLE I. The critical values g_c and ξ_c^* for different magnetic phases in the cases $N=\infty$ [see Eqs. (53), (55), and (58)] and $N=2$ in the approximation of Sec. III (i) and with account of the incoherent contribution (ii). The parameter values are $\lambda=5$, $\alpha=1/2$, $\delta=1/100$. For $N=2$, the ‘‘critical value’’ of ξ_c^* is estimated from the plateau in the dependence $\xi^*(g)$ (see the discussion in the text).

		PM	FM	3D AFM	2D AFM
$N \rightarrow \infty$	g_c	0.167	0.167	0.171	0.176
	ξ_c^*	–	–	5.35	5
$N=2$ (i)	g_c	0.154	0.139	0.132	0.127
	ξ_c^*	–	6.13	6.07	6.07
$N=2$ (ii)	g_c	0.154	0.141	0.136	0.131
	ξ_c^*	–	6.23	6.17	6.16

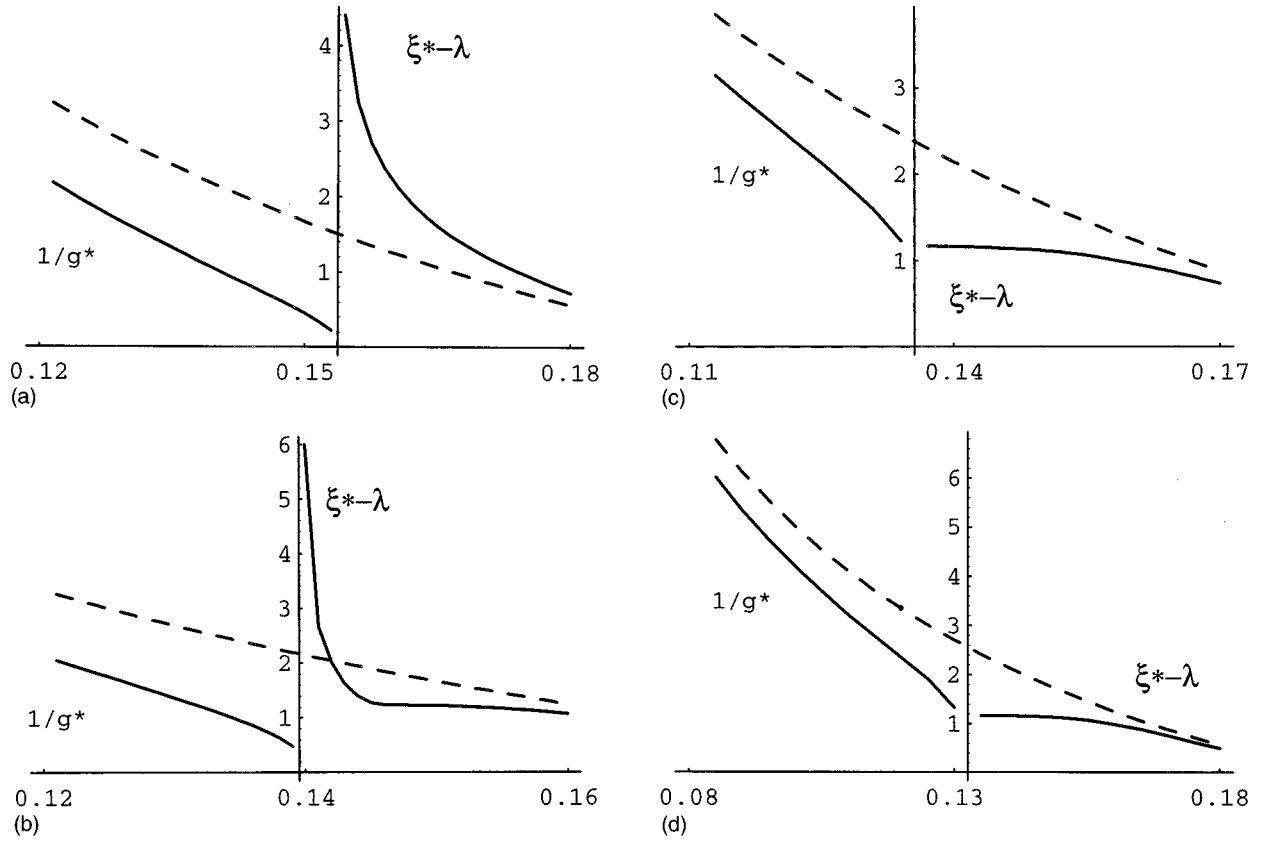


FIG. 5. The dependences $1/g^*(g)$ for $g < g_c$ and $\xi^*(g) - \lambda$ for $g > g_c$ in a paramagnet (a), ferromagnet (b), 3D antiferromagnet (c), and 2D antiferromagnet (d) according to Eq. (77). The dashed line is the curve $1/g - \lambda$, $\lambda = 5$, $\alpha = 1/2$, $N = 2$. In the magnetically ordered phases we set $\delta = 1/100$.

show the above-discussed increase of $1/g^*$ and ξ^* in the AFM case, which takes place at very small $|g - g_c|$. The experimentally observable quantities can be obtained from these data by using the formulas

$$S^* = \bar{S}_{ef}(C=0) = S \exp(-(V/N)[g^* - g]), \quad (80)$$

$$\bar{\omega}^* = \bar{\omega}_{ef}(C=0) = \bar{\omega} \exp(-(aV/N)[g^* - g]),$$

($g < g_c$). For $g > g_c$ we have

$$T_K^* = D \exp(-\xi^*). \quad (81)$$

One can see from Fig. 5 that, provided that g is far from g_c , we have the one-impurity behavior $\xi^*(g) \approx 1/g$, and the dependence $1/g^*(g)$ is given by Eqs. (52) and (54), as well as in the large- N limit.

VII. CRITICAL BEHAVIOR ON THE BOUNDARY OF THE STRONG-COUPLING REGIME: BREAKDOWN OF THE FERMI-LIQUID PICTURE

To investigate the ‘‘critical’’ behavior of ξ^* at $g \rightarrow g_c$ we consider the function $1/g_{ef}(g, C)$ at small $|g - g_c|, |C|$. First we consider the results of the solution of Eq. (62). With approaching g_c , the ξ region, where the behavior (64) takes place, becomes very narrow and not too important for determining ξ^* . Unlike the exponential (in ξ) behavior in the large- N limit, we have from Eq. (72),

$$g_{ef}(g = g_c, \xi \rightarrow \infty) \approx -(N/Va)\xi. \quad (82)$$

However, the dependence $\xi^*(g)$ turns out to be qualitatively the same as for $N \rightarrow \infty$ [see Eq. (57)],

$$\xi^* \approx \gamma \ln(g - g_c). \quad (83)$$

Numerical calculations yield $\gamma = 1/2$ for the FM at $N = 2$, and $\gamma = 1$ for the FM with $N > 2$ and PM. These values are the same as for $a \rightarrow 0$ [or as according to the large- N equation (44), provided that we take for the FM function (50)]. Thus one may put forward the hypothesis that the critical exponents are universal, i.e., depend on the type of magnetic ordering only, but not on N , V , and α . In the AFM phases numerical calculations yield the dependences (83) with $\gamma \approx 0.1$ ($d = 3$) and $\gamma \approx 10^{-3}$ ($d = 2$).

At the same time, the behavior of g^* at $g \rightarrow g_c - 0$ changes in comparison with the large- N limit. It turns out that for finite N one may establish a scaling relation of relevant variables at $g > g_c$ and $g < g_c$, as well as in the standard theory of critical phenomena. To find this relation, we consider our problem in the region $|g - g_c| > \varepsilon$ where $\varepsilon \rightarrow 0$ determines a scale of approaching to the critical point. When crossing the cut region, the argument of function Ψ should not shift considerably (Figs. 2 and 3). Indeed, this argument must be close to zero; in the ordered phases it is fixed by the singularity point, and for PM a considerable ‘‘smearing’’ takes place. Then we may estimate

$$\lambda + (aV/N)[g^* - g] \approx \xi^*, \quad (84)$$

so that

$$g^* \approx \gamma(N/Va) \ln(g_c - g). \quad (85)$$

As demonstrated by numerical calculations [Fig. 5(a)], in the PM phase the increase of $1/g^*$ for g not too close to g_c is almost linear in g , as well as in the large- N limit, and the behavior (85) takes place only starting from $g^* \sim 10$ which is, strictly speaking, beyond the applicability of the lowest-order scaling. At the same time, for the FM case the logarithmic dependence takes place in a considerable interval of $1/g^*$. As discussed in the previous section, for 2D AFM's the increase of g^* and ξ^* at $g \rightarrow g_c$ can be hardly observed.

Of course, for 3D AFM's $g_c^* = 1/\Delta$ is in fact finite, and the behavior (85) takes place at not too large g^* . More exactly, we can write down

$$1/g^* \approx 1[\gamma(N/Va) \ln(g_c - g)] + \Delta. \quad (86)$$

However, practically the ‘‘saturation’’ region is extremely narrow and cannot be achieved because of the smallness of γ .

When taking into account the incoherent contribution, a crossover to a PM-like regime takes place at $g \rightarrow g_c$ in the dependences $g^*(g)$ and $\xi^*(g)$, so that at very small $|g - g_c|$ we have the behavior of Eqs. (83) and (85) with $\gamma = 1$.

Basing on the results of Eqs. (83) and (85), it is natural to assume that at $g \rightarrow g_c$, $C \rightarrow -0$ one has the scaling behavior

$$g_{ef}(g, C) = -(N\gamma/aV) \ln(|C/\bar{\omega}|^{1/\gamma} + B(g_c - g)/g), \quad (87)$$

($B > 0$ is a constant, the argument of the logarithm should be positive). Then, according to Eqs. (60) and (61)

$$\bar{\omega}_{ef}(g, C)/\bar{\omega} \sim [|C/\bar{\omega}|^{1/\gamma} + B(g_c - g)/g]^\gamma, \quad (88)$$

$$\bar{S}_{ef}(g, C)/S \sim [|C/\bar{\omega}|^{1/\gamma} + B(g_c - g)/g]^{\gamma/a}. \quad (89)$$

In particular, we have at $g \rightarrow g_c$ the power-law dependences

$$T_K^*, \bar{\omega}^* \sim [\pm (g - g_c)]^\gamma, \quad (90)$$

$$S^* \sim (g_c - g)^{\gamma/a}. \quad (91)$$

Thus the ‘‘critical exponents’’ for the characteristic energy scales, namely, for T_K^* at $g > g_c$ and $\bar{\omega}^*$ at $g < g_c$ coincide. Using Eq. (89) we obtain at $g = g_c$, $C \rightarrow 0$

$$\frac{\bar{S}_{ef}(C)}{S} = \left(\frac{\bar{\omega}_{ef}(C)}{\bar{\omega}} \right)^{1/a} \sim |C|^{\gamma/a}. \quad (92)$$

One of the most interesting consequences of our picture is a possibility of a non-Fermi-liquid behavior on the boundary of the strong-coupling region. Indeed, during the renormalization process at $C \rightarrow 0$ the effective spin-fluctuation frequency tends to zero, and the corresponding spectral density is concentrated near $\omega = 0$. In this sense, the situation is close to that in the one-impurity two-channel Kondo problem where a collective mode with zero frequency occurs, which leads to a breakdown of the Fermi-liquid picture due to elec-

tron scattering by this ‘‘ultrasoft’’ mode.¹⁹ Unfortunately, our perturbation approach does not permit us to determine explicitly the temperature dependences of observables since the coupling constant is not small in this regime. However, the calculations can be performed within the large- $[l]$ s - f model (see the next section).

Of course, vanishing of $\bar{\omega}_{ef}(C)$ at $|C| = T_K^*$ and of T_K^* and $\bar{\omega}^*$ at $g = g_c$ is the result of using the lowest-order perturbation theory at the derivation of the renormalization-group equations. In fact, one may expect that in the strong-coupling region $\bar{\omega}_{ef}(C) \sim T_K$.^{10,11} One may assume that the true scaling behavior, which may be continued into the strong-coupling region, differs from the lowest-order scaling behavior by the replacement

$$B(g - g_c)/g \rightarrow (T_K^*/\bar{\omega})^{1/\gamma}. \quad (93)$$

A scaling law, which is more general than Eq. (88), could be expected to have the form

$$\bar{\omega}_{ef}(C)/\bar{\omega} = (T_K^*/\bar{\omega}) \phi(C/T_K^*). \quad (94)$$

Then one has

$$\bar{S}_{ef}(C)/S = \psi(\bar{\omega}_{ef}(C)/\bar{\omega}). \quad (95)$$

A detailed investigation of magnetic properties (in particular, of the formation of small moments, which are characteristic for heavy-fermion systems) reduces to determining an explicit form of the functions ϕ and ψ . This problem cannot be solved within perturbative approaches.

VIII. THE NON-FERMI-LIQUID BEHAVIOR IN THE DEGENERATE s - f MODEL

As we have seen in Sec. V, in the large- N limit the renormalization of magnetic characteristics is weak in comparison with that of the electron spectrum. An opposite situation occurs in the case of large $[l]$ where the number of electron branches is much larger than that of spin-wave modes, so that the renormalization of spin dynamics plays the crucial role.

It is instructive to consider the large- l limit in the s - f model ($N=2$) with

$$[l] \rightarrow \infty, \quad g \rightarrow 0, \quad [l]g^2/2 = \tilde{g}^2 = \text{const.}$$

Then the effective s - f interaction is unrenormalized, $\tilde{g}_{ef} = \tilde{g} = \text{const}$, and the scaling equation takes the form

$$\frac{\partial \chi}{\partial \xi} = a \tilde{g}^2 \Psi(\lambda + \chi - \xi), \quad (96)$$

where

$$\chi(\xi) = \ln \frac{\bar{\omega}}{\bar{\omega}_{ef}(\xi)}.$$

When taking into account the incoherent contribution we obtain instead of Eq. (96)

$$\frac{\partial \chi}{\partial \xi} = a \tilde{g}^2 [Z \Psi_{\text{coh}}(\lambda + \chi - \xi) + (1 - Z) \Psi_{\text{incoh}}(\lambda + \chi - \xi)], \quad (97)$$

$$Z = 1/(1 + \chi/a).$$

By introducing the function

$$\nu = \lambda + \chi - \xi = \ln \frac{|C|}{\bar{\omega}_{ef}}, \quad (98)$$

Eq. (96) can be readily integrated to obtain

$$\int_{\nu}^{\lambda} \frac{d\xi'}{1 - a \tilde{g}^2 \Psi(\xi')} = \xi. \quad (99)$$

However, a simple qualitative analysis can be performed immediately for both Eqs. (96) and (97).

In the PM phase we have

$$\chi(\xi) \approx a \tilde{g}^2 \xi \quad (100)$$

up to the point

$$\xi_1 = \frac{\lambda}{1 - a \tilde{g}^2}. \quad (101)$$

Thus a power-law behavior occurs

$$\bar{\omega}_{ef}(C) \approx \bar{\omega}(|C|/D)^{\beta}, \quad \beta = a \tilde{g}^2. \quad (102)$$

For $\xi > \xi_1$,

$$\chi(\xi) \approx \chi(\xi_1) = \lambda a \tilde{g}^2 (1 - a \tilde{g}^2)^{-1} \quad (103)$$

is practically constant.

Note that unlike the case $l=0$, which was discussed in the previous section, the bare coupling constant \tilde{g} and the exponent β can be sufficiently large. At $\tilde{g} \sim 1$, $\bar{\omega}_{ef}(\xi)$ decreases rather rapidly during the renormalization process. Thus a ‘‘soft-mode’’ situation occurs, which may lead to a NFL behavior.

To investigate modification of the electron spectrum we may calculate the second-order perturbation theory corrections, which are formally small in $1/[l]$. Replacing $\bar{\omega} \rightarrow \bar{\omega}_{ef}(C)$ in the usual second-order result for the electron self-energy (cf. Ref. 33) and introducing the effective electron density of states at the Fermi level $N_{ef}(C)$ we obtain

$$N_{ef}(C) \sim \frac{Z(C)}{\bar{\omega}_{ef}(C)} \sim \left(\frac{D}{|C|} \right)^{\beta} \frac{D}{\ln |C|}. \quad (104)$$

To investigate qualitatively temperature dependences we may replace $|C| \rightarrow T$. Thus one may expect an essentially NFL behavior of the electronic specific heat,

$$C_e(T) \sim T N_{ef}(|C| \rightarrow T) \sim T^{1-\beta} \ln(D/T), \quad (105)$$

magnetic susceptibility,

$$\chi_m(T) \sim S_{ef}^2(|C| \rightarrow T)/T \sim 1/T^{1-\beta/a}, \quad (106)$$

transport properties, etc.

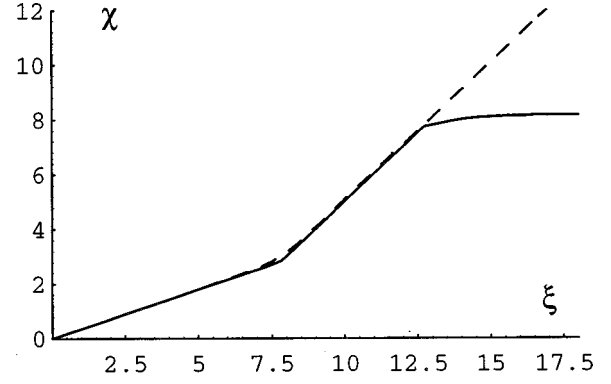


FIG. 6. The dependence of $\chi = \ln(\bar{\omega}/\bar{\omega}_{ef})$ vs $\xi = \ln|D/C|$ for a 2D antiferromagnet at $[l] = \infty$ with $\delta = 10^{-3}$, $\lambda = 5$, $\tilde{g} = 0.6$ according to Eq. (96) (dashed line) and with account of the incoherent contribution (solid line).

In magnetically ordered phases, the situation for $\xi > \xi_1$ changes since the singularity of $\Psi_{\text{coh}}(\xi)$ plays an important role. Provided that $a \tilde{g}^2 \Psi_{\text{coh}}^{\text{max}} > 1$, the argument of the function Ψ_{coh} at $\xi > \xi_1$ becomes almost constant, and we obtain

$$\chi(\xi) \approx \xi - \lambda, \quad \bar{\omega}_{ef}(C) \approx |C|. \quad (107)$$

The behavior (107) is similar to the dependence (88) for finite l , and corresponds to $g = g_c$. In the case of Eq. (96), this behavior takes place up to $\xi = \infty$. On the other hand, an account of the incoherent contribution results in that the increase of χ stops at $a \tilde{g}^2 \Psi_{\text{coh}}^{\text{max}} = 1/Z = 1 + \chi/a$, i.e., at

$$\xi_2 = \lambda + \chi_{\text{max}} = \lambda + a(a \tilde{g}^2 \Psi_{\text{coh}}^{\text{max}} - 1). \quad (108)$$

Thus the value of ξ_2 is determined by the quantity δ . The dependence $\chi(\xi)$ for a 2D antiferromagnet is shown in Fig. 6. In the presence of the incoherent contribution the region, where the dependence (107) holds, is rather narrow (especially for not too small δ). However, a more exact consideration of spin dynamics (rather than using the spin-diffusion approximation) may change considerably the results.

In the regime (107) we have the result (104) with $\beta = 1$ and $D \rightarrow \bar{\omega}$, so that in the AFM case ($a = 1$) one obtains

$$\chi_m(T) = \text{const}, \quad C_e(T) \sim \ln(\bar{\omega}/T). \quad (109)$$

For finite, but large $[l]$ the picture discussed fails below

$$T_K = D \exp(-[l]^{1/2}/\sqrt{2}\tilde{g}). \quad (110)$$

However, the NFL behavior takes place in a wide temperature region $T_K \ll T \leq \bar{\omega}$. At $T < T_K$ the renormalization of g_{ef} becomes important and, as discussed in the end of the previous section, a more complicated scaling behavior may take place.

As discussed in Sec. VI (see Fig. 4), a NFL behavior takes place even for $l=0$ for $g \approx g_c$. Numerical calculations confirm that the NFL region becomes broader with increasing $[l]$. The linear dependence $g_{ef}(\xi)$ with a small coefficient takes place up to $\xi \approx 5$, then this is changed by the linear ‘‘coherent’’ behavior which is further smeared by the incoherent contribution.

IX. CONCLUSIONS

In conclusion, we summarize the main results of our consideration, discuss their connection with peculiarities of the anomalous f -electron systems, and mention some unsolved problems. Three regimes are possible at $I < 0$ depending on the relation between the one-impurity Kondo temperature T_K and bare spin-fluctuation frequency $\bar{\omega}$: (i) The strong-coupling regime with $I_{ef}(C \rightarrow 0) \rightarrow \infty$ where all the conduction electrons are bound into singlet states and spin dynamics is suppressed. This regime is expected to occur provided that $\bar{\omega} \ll T_K$. (ii) The regime of a ‘‘Kondo’’ magnet with an appreciable, but not total compensation of magnetic moments, which corresponds to small $|g - g_c|$. (iii) The regime of ‘‘usual’’ magnets with small logarithmic corrections to the ground-state moment and $\bar{\omega}_{ef}$. (Note that the same situation takes place at $I > 0$.¹³)

The formation of magnetic state takes place at

$$T_K^c \equiv D \exp(-1/g_c) = A \bar{\omega} \left(\frac{\bar{\omega}}{D} \right)^{1/a_c - 1} \quad (111)$$

($a_c \equiv \lambda g_c$, A is of the order of unity). For $N \rightarrow \infty$ we have $a_c = 1 + O(1/\lambda)$ and the strong-coupling region boundary is determined by the condition $T_K = A \bar{\omega}$. For finite N we always have $a_c < 1$ (see Table I) and, according to Eq. (111), $T_K^c \ll \bar{\omega}$.

It should be stressed that the Doniach criterion $g_c \approx 0.4$,⁸ which was obtained for a very special case in a simplified one-dimensional model, cannot in fact be used for real systems. Indeed, as demonstrated by numerical calculations for $N = 2$, g_c turn out to be sensitive to parameters of exchange interactions, type of magnetic ordering, space dimensionality, degeneracy factors, etc.

It is a common practice to treat the interplay of spin dynamics and the Kondo effect within the two-impurity problem (see, e.g., Refs. 34). However, we have demonstrated that the most important features of the scaling behavior are connected with peculiarities of the spin spectral density and are not described by this model (where the spectral density is a δ -like peak corresponding to singlet-triplet transitions).

We have used in our calculations the simplest ‘‘Debye’’ approximation for the magnon spectrum, i.e., the long-wave dispersion law in the whole Brillouin zone. At the same time, competing interspin interactions, which are owing to the oscillating behavior of the RKKY exchange and can lead to frustrations, might be important for explaining magnetic structures in the ‘‘usual’’ Kondo lattices.

The effective Kondo temperature T_K^* determines a characteristic energy scale of the ‘‘heavy-fermion’’ behavior at low temperatures. This can differ considerably from the one-impurity value T_K , so that in the PM phase $T_K^* < T_K$, and in the magnetically ordered phases, except for very small $g - g_c$, $T_K^* > T_K$ (see Fig. 5). In the AFM case T_K^* depends weakly on g and therefore on T_K , and is determined by $\bar{\omega}$ in a wide interval of g .

Although our consideration was performed for $T = 0$, one may expect by analogy with the one-impurity problem that the dependences $\bar{S}(T)$ [in the PM phase, $\bar{S}(T)$ is the local

moment determined from the magnetic susceptibility] and $\bar{\omega}(T)$ may be qualitatively obtained by a simple replacement $|C| \rightarrow T$.

For $N = 2$ and small enough δ (spin excitation damping), the Kondo screening in the AFM and FM phases is stronger than in the PM phase. This leads to an increase of the Rhodes-Wohlfarth ratio (i.e., of the ratio of the effective moment, as determined from the Curie constant, to the saturation moment). For example, if the bare coupling constant is close to its critical value in the ordered phase and correspondingly lower than in the PM phase, the ground-state moment is small in comparison with the high-temperature one (a behavior, typical for most Kondo magnets, as well as weak itinerant electron d magnets). The same situation takes place for the characteristic spin-fluctuation frequency $\bar{\omega}_{ef}$. It should be noted that an increase of spin-fluctuation energies with temperature is indeed observed in a number of anomalous f -electron systems, e.g., U_2Zn_{17} .³⁵

Presence of the factor $1/N$ in the AFM2 case or a large value of δ (magnon damping) may result in that the suppression of the effective moment and spin-dynamics frequency turns out to be weaker than in the PM phase. It looks like the decrease of moment at magnetic disordering with increasing temperature. Such a decrease is typical for strong itinerant magnets, where it is due to the change of electron spectrum at disordering (see Refs. 28 and 36). In the case under consideration this phenomenon has a quite different (essentially many-particle) nature.

Near the boundary of the strong-coupling region ($g \rightarrow g_c$) the relevant variables demonstrate a nontrivial scaling behavior as functions of $|g - g_c|$ and ξ . In particular,

$$T_K^*(g \rightarrow g_c + 0), \bar{\omega}^*(g \rightarrow g_c - 0) \sim |g - g_c|^\gamma, \quad (112)$$

the exponent γ depending on the type of magnetic ordering. These results may be of interest for the general theory of metallic magnetism. The description of the state with small magnetic moment ($g \rightarrow g_c$) turns out to differ considerably from that in the theory of weak itinerant magnetism.³² It is interesting that the ‘‘critical exponents’’ in the dependences of the moment on the coupling constant (91) and C (92) turn out to be noninteger. The corresponding dependences $\bar{S}(T) = \bar{S}_{ef}(|C| \rightarrow T)$ describe an analog of the ‘‘temperature-induced magnetism.’’³²

As mentioned in the Introduction, high sensitivity of the magnetic state in heavy-fermion systems to external factors is explained by that in case (ii) the magnetic moment changes strongly at small variations of the bare coupling constant g . According to our consideration, the regime of small magnetic moments occurs in a very narrow region of bare parameters only. The renormalized values of magnetic moment and spin-fluctuation frequency are determined by the quantity g^* . Provided that g is not too close to g_c , a characteristic interval of the change of g^* by unity is estimated as $\delta g \sim g^2 \ll g$. In the immediate vicinity of g_c (where the behavior $g^* \sim -\ln|g - g_c|$ takes place) this interval becomes still more narrow: $\delta g \sim |g - g_c|$. A more consistent treatment of this regime with account of possible renormalization of the scale $|g - g_c|$ itself requires using more complicated (e.g., numerical) scaling approaches.

“Softening” of the spin excitation spectrum in the critical region may result in a non-Fermi-liquid behavior. Although the NFL state itself cannot be described within the framework of our perturbative approach, the conclusion about the NFL behavior near the boundary of magnetic ($g < g_c$) and nonmagnetic ($g > g_c$) phases seems to be important. This conclusion is confirmed by the fact that a violation of the Fermi-liquid picture in the anomalous f -electron system is really observed near the onset of magnetic ordering.¹⁴ It is difficult to explain this fact within the frequently used one-impurity two-channel Kondo model.¹⁷ At the same time, our scenario of the NFL state formation takes into account essentially the *many-center* nature of the system. The width of the region where the NFL behavior occurs increases with increasing the degeneracy factor [I] and decreases with increasing N . In the formal limit [I] $\rightarrow \infty$ perturbation theory in g remains applicable, so that explicit expressions for thermodynamic and magnetic properties can be obtained.

On the whole, the physical behavior that occurs as a result of an interplay between the Kondo effect and intersite exchange interactions, turns out to be very rich and differs for various model versions.

ACKNOWLEDGMENT

The work was supported in part by Grant No. 96-02-16000 from the Russian Basic Research Foundation.

APPENDIX A: GROUND STATE AND SPECTRUM OF SPIN EXCITATIONS OF THE LOCALIZED-SPIN SYSTEM IN MODELS (2) AND (7)

In the ground ferromagnetic (FM) state of model (2) to zeroth approximation in I we have $\langle S_i^z \rangle = S$, and the spin-wave spectrum reads

$$\omega_{\mathbf{q}} = \omega_{\mathbf{q}}^{\text{FM}}(S) = 2S(J_{\mathbf{q}} - J_0). \quad (\text{A1})$$

For model (7), we also assume the magnon character of spin dynamics. Then the spin-wave spectrum can be found by linearizing the equation of motion for the “spin-deviation” operator $X_{-\mathbf{q}}^{MS}$. There exist $2S = N - 1$ spin-wave modes with the frequency $\omega_{\mathbf{q}} = \omega_{\mathbf{q}}^{\text{FM}}(1/2)$, which correspond to the transitions $S \rightarrow M < S$.

Now we discuss an antiferromagnet which has the spiral structure along the x axis with the wave vector \mathbf{Q} ($J_{\mathbf{Q}} = J_{\min}$)

$$\langle S_i^z \rangle = S \cos \mathbf{Q} \mathbf{R}_i, \quad \langle S_i^y \rangle = S \sin \mathbf{Q} \mathbf{R}_i, \quad \langle S_i^x \rangle = 0.$$

We introduce the local coordinate system

$$S_i^z = \hat{S}_i^z \cos \mathbf{Q} \mathbf{R}_i - \hat{S}_i^y \sin \mathbf{Q} \mathbf{R}_i, \quad (\text{A2})$$

$$S_i^y = \hat{S}_i^y \cos \mathbf{Q} \mathbf{R}_i + \hat{S}_i^z \sin \mathbf{Q} \mathbf{R}_i, \quad S_i^x = \hat{S}_i^x.$$

Hereafter we consider for simplicity a two-sublattice AFM ($2\mathbf{Q}$ is equal to a reciprocal-lattice vector, so that $\cos^2 \mathbf{Q} \mathbf{R}_i = 1$, $\sin^2 \mathbf{Q} \mathbf{R}_i = 0$). Passing to the spin-deviation operator we represent the standard Heisenberg Hamiltonian in the spin-wave region as

$$H_f = \text{const} + \sum_{\mathbf{q}} \left[C_{\mathbf{q}} b_{\mathbf{q}}^{\dagger} b_{\mathbf{q}} + \frac{1}{2} D_{\mathbf{q}} (b_{-\mathbf{q}} b_{\mathbf{q}} + b_{\mathbf{q}}^{\dagger} b_{-\mathbf{q}}^{\dagger}) \right], \quad (\text{A3})$$

$$C_{\mathbf{q}} = S(J_{\mathbf{Q}+\mathbf{q}} + J_{\mathbf{q}} - 2J_{\mathbf{Q}}), \quad D_{\mathbf{q}} = S(J_{\mathbf{q}} - J_{\mathbf{Q}+\mathbf{q}}).$$

Diagonalizing Eq. (A3) we obtain the spin-wave spectrum

$$\omega_{\mathbf{q}} = \omega_{\mathbf{q}}^{\text{AFM}}(S) = (C_{\mathbf{q}}^2 - D_{\mathbf{q}}^2)^{1/2} = 2S(J_{\mathbf{q}} - J_{\mathbf{Q}})^{1/2} (J_{\mathbf{Q}+\mathbf{q}} - J_{\mathbf{Q}})^{1/2}. \quad (\text{A4})$$

The corresponding transformation to the local coordinate system for model (7) has the form

$$X_i^{MM'} = \frac{1}{2} [\hat{X}_i^{M,M'} (1 + \cos \mathbf{Q} \mathbf{R}_i) + \hat{X}_i^{-M,-M'} (1 - \cos \mathbf{Q} \mathbf{R}_i)].$$

Then we obtain

$$H_f = \sum_{\mathbf{q}} \sum_{M,M'=-S}^S (J_{\mathbf{q}}^{(2)} \hat{X}_{-\mathbf{q}}^{MM'} \hat{X}_{\mathbf{q}}^{M'M} + J_{\mathbf{q}}^{(1)} \hat{X}_{-\mathbf{q}}^{MM'} \hat{X}_{\mathbf{q}}^{-M'-M}), \quad (\text{A5})$$

$$H_{sf} = -\frac{1}{2} I \sum_{\mathbf{k}\mathbf{q}} \sum_{M,M'=-S}^S [(\hat{X}_{\mathbf{q}}^{M,M'} + \hat{X}_{\mathbf{q}}^{-M,-M'}) + (\hat{X}_{\mathbf{q}+\mathbf{Q}}^{M,M'} - \hat{X}_{\mathbf{q}+\mathbf{Q}}^{-M,-M'})] c_{\mathbf{k}M}^{\dagger} c_{\mathbf{k}-\mathbf{q}M} \quad (\text{A6})$$

with

$$J_{\mathbf{q}}^{(1,2)} = \frac{1}{2} (J_{\mathbf{q}} \mp J_{\mathbf{q}+\mathbf{Q}}).$$

In the mean-field approximation we have

$$\langle H_f \rangle = \sum_{M=-S}^S (J_0^{(2)} n_M^2 + J_0^{(1)} n_M n_{-M}) \quad (\text{A7})$$

with $n_M = \langle \hat{X}_i^{MM} \rangle$. The usual AFM state turns out to be unstable for simple lattices provided that only the nearest-neighbor interaction is taken into account ($J_{\mathbf{q}}^{(2)} \equiv 0$). Indeed, in this case any state with

$$\sum_{M>0} n_M = 1, \quad \sum_{M<0} n_M = 0$$

has the same energy $\langle H_f \rangle = 0$. When introducing the next-neighbor ferromagnetic interaction ($J_0^{(2)} < 0$) the AFM state with

$$n_S = 1, \quad n_{M<S} = 0 \quad (\text{A8})$$

is stabilized. This state will be referred to as AFM1. The corresponding “spin-wave” spectrum contains N branches. The mode, which corresponds to the transition $S \rightarrow -S$, has the frequency $\omega_{\mathbf{q}}^{(a)} = \omega_{\mathbf{q}}^{\text{AFM}}(S = 1/2)$. Other $N - 2$ modes have a ferromagnetic type and possess the energy

$$\omega_{\mathbf{q}}^{(f)} = \omega_{\mathbf{q}}^{\text{FM}}(S = 1/2, J_{\mathbf{q}} \rightarrow J_{\mathbf{q}}^{(2)}).$$

Provided that the next-neighbor interaction is antiferromagnetic too ($J_0^{(2)} > 0$), this case is referred to as AFM2), minimization of Eq. (A7) yields

$$n_{M<0}=0, \quad n_{M>0}=K \equiv \begin{cases} 2/N=2/(2S+1), & N \text{ even} \\ J_0/(SJ_0+J_0^{(2)}), & N \text{ odd.} \end{cases} \quad (\text{A9})$$

For odd N we have

$$n_0=J_0^{(2)}/(SJ_0+J_0^{(2)}) \approx J_0^{(2)}/(SJ_0) \ll K. \quad (\text{A10})$$

Then, according to Eq. (9), for $N>2$ the sublattice magnetization turns out to be reduced in comparison with S already in the mean-field approximation:

$$\bar{S} = \frac{1}{2} \times \begin{cases} S+1/2, & S \text{ half-integer} \\ (S+1)(1-n_0), & S \text{ integer.} \end{cases} \quad (\text{A11})$$

Then there exist $N^2/4$ (N even) or $(N-1)^2/4$ (N odd) ‘‘antiferromagnetic’’ modes which correspond to the transitions from $M>0$ to $M'<0$ and have the frequency $\omega_{\mathbf{q}}^{(a)} = \omega_{\mathbf{q}}^{\text{AFM}}(S=K)$. Besides that, for odd N there exist peculiar modes with the frequencies $\omega_{\mathbf{q}}^{\Omega}$, which describe the transitions $M \rightarrow 0$ and are determined by the equations

$$\Omega_{\mathbf{q}}^{\pm}(\omega) \equiv [\omega \mp (K-2n_0)C_{\mathbf{q}}](\omega \pm n_0C_{\mathbf{q}}) + n_0(K-2n_0)D_{\mathbf{q}}^2 = 0 \quad (\text{A12})$$

(the plus sign corresponds to $M>0$ and the minus sign to $M<0$), so that to lowest order in n_0

$$\omega_{\mathbf{q}1}^{\Omega_{\pm}} \approx \pm KC_{\mathbf{q}}, \quad \omega_{\mathbf{q}2}^{\Omega_{\pm}} \approx \mp n_0(C_{\mathbf{q}}^2 - D_{\mathbf{q}}^2)/C_{\mathbf{q}}. \quad (\text{A13})$$

Thus one of the solutions to Eq. (A12) describes the mode which is very soft for $J_0^{(2)} \ll SJ_0$. Since the Kondo singular contributions, which are cut at this mode, are large, this may result in a tendency to the destruction of magnetism.

Really, the considered ground states and excitation spectra are strongly influenced by the crystal field.^{21,37,38} In particular, large gaps and degeneracy lift may occur in the above-discussed ‘‘additional’’ modes. This question needs special consideration.

APPENDIX B: RENORMALIZATIONS IN THE PARAMAGNETIC PHASE

The Kondo-lattice problem in the paramagnetic state describes the process of screening of localized magnetic moments that are determined from the temperature dependence of magnetic susceptibility, and the related anomalies in the electron spectrum and damping.

To find the renormalization of the effective s - f exchange parameter we consider the electron self-energy. In the second order in I we have

$$\Sigma_{\mathbf{k}}^{(2)}(E) = I^2 P \sum_{\mathbf{q}} \frac{1}{E - t_{\mathbf{k}-\mathbf{q}}}, \quad (\text{B1})$$

where

$$P = \begin{cases} [I]S(S+1), & \text{model (2)} \\ 1 - 1/N^2, & \text{model (7)}. \end{cases} \quad (\text{B2})$$

To construct a self-consistent theory of Kondo lattices, we have to calculate the third-order Kondo correction to the self-energy with account of spin dynamics. Such calculations

were performed in Refs. 9 within the simplest nondegenerate s - f model. Repeating a similar procedure in a more general case we obtain for the singular contribution (which contains a logarithmic divergence in the absence of spin dynamics)

$$\Sigma_{\mathbf{k}}^{(3)}(E) = -I^3 P N \int_{-\infty}^{\infty} d\omega \sum_{\mathbf{q}, \mathbf{p}} \mathcal{J}_{\mathbf{q}}(\omega) \frac{n_{\mathbf{k}-\mathbf{q}}}{E - t_{\mathbf{k}-\mathbf{q}} - \omega} \times \left(\frac{1}{E - t_{\mathbf{k}-\mathbf{p}}} - \frac{1}{t_{\mathbf{k}-\mathbf{q}} - t_{\mathbf{k}-\mathbf{p}}} \right), \quad (\text{B3})$$

where $N=2$ in model (2), the spin dynamics is neglected in the denominator which is not connected with the Fermi function $n_{\mathbf{k}} = n(t_{\mathbf{k}})$,

$$\mathcal{J}_{\mathbf{q}}(\omega) = -\frac{1}{\pi} N(\omega) \frac{\text{Im} \langle \langle S_{\mathbf{q}}^z | S_{-\mathbf{q}}^z \rangle \rangle_{\omega}}{\langle S_{-\mathbf{q}}^z S_{\mathbf{q}}^z \rangle} \quad (\text{B4})$$

is the spectral density of the spin Green's function for the Hamiltonian H_f , which is normalized to unity, $N(\omega)$ being the Bose function. The Kondo renormalization of the s - f parameter $I \rightarrow I_{ef} = I + \delta I_{ef}$ is determined by ‘‘including’’ $\text{Im} \Sigma_{\mathbf{k}}^{(3)}(E)$ into $\text{Im} \Sigma_{\mathbf{k}}^{(2)}(E)$, and is given by

$$\delta I_{ef} = -\frac{N}{2} I^2 \int_{-\infty}^{\infty} d\omega \sum_{\mathbf{q}} \mathcal{J}_{\mathbf{q}}(\omega) \frac{n_{\mathbf{k}-\mathbf{q}}}{E - t_{\mathbf{k}-\mathbf{q}} - \omega} \quad (\text{B5})$$

(we have to set $E = E_F = 0$, $k = k_F$ in the expressions for I_{ef}). To concretize the form of spin dynamics in the paramagnetic phase we use the spin-diffusion approximation

$$\mathcal{J}_{\mathbf{q}}(\omega) = \frac{1}{\pi} \frac{\mathcal{D}q^2}{\omega^2 + (\mathcal{D}q^2)^2} \quad (\text{B6})$$

(\mathcal{D} is the spin-diffusion constant) which is correct at small \mathbf{q}, ω and is reasonable in a general case. Then we derive

$$\delta I_{ef} = -\frac{N}{2} I^2 \text{Re} \sum_{\mathbf{q}} \frac{n_{\mathbf{k}-\mathbf{q}}}{E - t_{\mathbf{k}-\mathbf{q}} - i\mathcal{D}q^2}. \quad (\text{B7})$$

To calculate the correction to the effective magnetic moment we treat the static magnetic susceptibility

$$\chi = \langle S^z, S^z \rangle \equiv \int_0^{1/T} d\lambda \langle \exp(\lambda H) S^z \exp(-\lambda H) S^z \rangle. \quad (\text{B8})$$

Expanding to second order in I we derive (cf. Ref. 9)

$$\chi = \bar{S}_{ef}^2 / 3T, \quad \bar{S}_{ef}^2 = S(S+1)[1-L], \quad (\text{B9})$$

$$L = 2RI^2 \int_{-\infty}^{\infty} d\omega \sum_{\mathbf{k}, \mathbf{q}} \mathcal{J}_{\mathbf{q}}(\omega) \frac{n_{\mathbf{k}}(1-n_{\mathbf{k}-\mathbf{q}})}{(t_{\mathbf{k}} - t_{\mathbf{k}-\mathbf{q}} - \omega)^2}$$

where we have introduced the notation

$$R = \begin{cases} [I], & \text{model (2)} \\ N/2, & \text{model (7)}. \end{cases} \quad (\text{B10})$$

The spin-fluctuation frequency in the paramagnetic phase is determined from the second moment of the spin Green's function

$$\omega_{\mathbf{q}}^2 = (\dot{S}_{-\mathbf{q}}^z, \dot{S}_{\mathbf{q}}^z) / (S_{-\mathbf{q}}^z, S_{\mathbf{q}}^z). \quad (\text{B11})$$

To second order in I we derive (cf. Refs. 10 and 13)

$$(\omega_{\mathbf{q}}^2)_0 = \frac{4}{3} S(S+1) \sum_{\mathbf{p}} (J_{\mathbf{q}-\mathbf{p}} - J_{\mathbf{p}})^2, \quad (\text{B12})$$

$$\delta\omega_{\mathbf{q}}^2 / \omega_{\mathbf{q}}^2 = (1 - \tilde{\alpha}_{\mathbf{q}}) \delta\bar{S}_{ef}^2 / \bar{S}_{ef}^2 = -(1 - \tilde{\alpha}_{\mathbf{q}}) L, \quad (\text{B13})$$

where we have taken into account spin dynamics by analogy with Eq. (B9). Passing into real space yields for the quantity $\tilde{\alpha}_{\mathbf{q}}$

$$\tilde{\alpha}_{\mathbf{q}} = \sum_{\mathbf{R}} J_{\mathbf{R}}^2 \left(\frac{\sin k_{\mathbf{F}} R}{k_{\mathbf{F}} R} \right)^2 [1 - \cos \mathbf{q} \mathbf{R}] / \sum_{\mathbf{R}} J_{\mathbf{R}}^2 [1 - \cos \mathbf{q} \mathbf{R}]. \quad (\text{B14})$$

This quantity differs from the result for a ferromagnet (19) by the replacement $J_{\mathbf{R}} \rightarrow J_{\mathbf{R}}^2$. However, in the nearest-neighbor approximation we obtain the same result (20).

APPENDIX C: EFFECTIVE s - f INTERACTION IN MAGNETICALLY ORDERED PHASES

Here we investigate the renormalization of the s - f interaction in the FM and AFM phases. First we treat model (2). For a ferromagnet the electron spectrum possesses the spin splitting, $E_{\mathbf{k}\sigma} = t_{\mathbf{k}} - \sigma[I]IS$. The second-order correction to I_{ef} is determined by the corresponding electron self-energies (cf. Ref. 9):

$$\delta I_{ef} = -[\Sigma_{\mathbf{k}\uparrow}^{\text{FM}}(E) - \Sigma_{\mathbf{k}\downarrow}^{\text{FM}}(E)] / (2S[I]) \quad (\text{C1})$$

with

$$\begin{aligned} \Sigma_{\mathbf{k}\uparrow}^{\text{FM}}(E) &= 2RI^2 S \sum_{\mathbf{q}} \frac{n_{\mathbf{k}-\mathbf{q}}}{E - t_{\mathbf{k}-\mathbf{q}} + \omega_{\mathbf{q}}^{\text{FM}}}, \\ \Sigma_{\mathbf{k}\downarrow}^{\text{FM}}(E) &= 2RI^2 S \sum_{\mathbf{q}} \frac{1 - n_{\mathbf{k}-\mathbf{q}}}{E - t_{\mathbf{k}-\mathbf{q}} - \omega_{\mathbf{q}}^{\text{FM}}}. \end{aligned} \quad (\text{C2})$$

For an antiferromagnet the electron spectrum contains the AFM gap,

$$E_{\mathbf{k}} = \frac{1}{2} (t_{\mathbf{k}} + t_{\mathbf{k}+\mathbf{Q}}) \pm \left[\frac{1}{4} (t_{\mathbf{k}} - t_{\mathbf{k}+\mathbf{Q}})^2 + ([I]IS)^2 \right]^{1/2}. \quad (\text{C3})$$

The renormalization of I is obtained from the second-order correction to the anomalous Green's function

$$\langle\langle c_{\mathbf{k}\sigma} | c_{\mathbf{k}+\mathbf{Q}\sigma}^\dagger \rangle\rangle_E = -\sigma \frac{[I]IS - \Sigma_{\mathbf{k}, \mathbf{k}+\mathbf{Q}}^{\text{AFM}}(E)}{(E - t_{\mathbf{k}})(E - t_{\mathbf{k}+\mathbf{Q}})},$$

so that

$$\delta I_{ef} = -\Sigma_{\mathbf{k}, \mathbf{k}+\mathbf{Q}}^{\text{AFM}}(E) / (S[I]). \quad (\text{C4})$$

The calculation of the off-diagonal self-energy gives

$$\Sigma_{\mathbf{k}, \mathbf{k}+\mathbf{Q}}^{\text{AFM}}(E) = 2RI^2 S \sum_{\mathbf{q}} \frac{n_{\mathbf{k}-\mathbf{q}}(E - t_{\mathbf{k}-\mathbf{q}})}{(E - t_{\mathbf{k}-\mathbf{q}})^2 - (\omega_{\mathbf{q}}^{\text{AFM}})^2}. \quad (\text{C5})$$

To calculate the corrections to I_{ef} in the Coqblin-Schrieffer model we consider the Green's function

$$\sum_{M>0} (\langle\langle c_{\mathbf{k}M} | c_{\mathbf{k}+\mathbf{Q}M}^\dagger \rangle\rangle_E - \langle\langle c_{\mathbf{k}, -M} | c_{\mathbf{k}+\mathbf{Q}, -M}^\dagger \rangle\rangle_E), \quad (\text{C6})$$

which determines the ‘‘magnetization’’ (FM case, $\mathbf{Q}=0$) or ‘‘staggered magnetization’’ (AFM case) of conduction electrons.

For a ferromagnet the mean-field electron spectrum reads $E_{\mathbf{k}M} = t_{\mathbf{k}} - I\delta_{MS}$. Calculating the second-order corrections we derive

$$\delta I_{ef} = -2[(N-1)\Sigma_{\mathbf{k}\uparrow}^{\text{FM}}(E) - \Sigma_{\mathbf{k}\downarrow}^{\text{FM}}(E)] / N \quad (\text{C7})$$

(remember that in the Coqblin-Schrieffer model the self-energies should be substituted at $S=1/2$).

In the AFM1 state the mean-field electron spectrum for $M=S, -S$ is given by Eq. (C3) with the replacement $t_{\mathbf{k}} \rightarrow t_{\mathbf{k}} - I$. For other M the spectrum is unrenormalized. The renormalization of I in such a situation contains contributions of both FM and AFM types:

$$\begin{aligned} \delta I_{ef} &= -2[(N-2)\Sigma_{\mathbf{k}\uparrow}^{\text{FM}}(E, \omega_{\mathbf{q}}^{\text{FM}} \rightarrow \omega_{\mathbf{q}}^{(f)}) \\ &\quad + \Sigma_{\mathbf{k}, \mathbf{k}+\mathbf{Q}}^{\text{AFM}}(E, \omega_{\mathbf{q}}^{\text{AFM}} \rightarrow \omega_{\mathbf{q}}^{(a)})] / N. \end{aligned} \quad (\text{C8})$$

In the case AFM2 the electron spectrum is given by Eq. (C3) with $S \rightarrow K/2$, $t_{\mathbf{k}} \rightarrow t_{\mathbf{k}} - IK$. Besides that, for odd N there exists a branch of spectrum with $M=0$, which is weakly renormalized due to smallness of $|J_0^{(2)}|$. Then we obtain for even N

$$\delta I_{ef} = -2\Sigma_{\mathbf{k}, \mathbf{k}+\mathbf{Q}}^{\text{AFM}}(E, \omega_{\mathbf{q}}^{\text{AFM}} \rightarrow \omega_{\mathbf{q}}^{(a)}). \quad (\text{C9})$$

For odd N the contribution of the mode Eq. (A12) occurs:

$$\begin{aligned} \delta I_{ef} &= -2\frac{N-1}{N}\Sigma_{\mathbf{k}, \mathbf{k}+\mathbf{Q}}^{\text{AFM}}(E, \omega_{\mathbf{q}}^{\text{AFM}} \rightarrow \omega_{\mathbf{q}}^{(a)}) \\ &\quad - [(K - n_0)\Sigma_{\mathbf{k}, \mathbf{k}+\mathbf{Q}}^{\Omega+}(E) + n_0\Sigma_{\mathbf{k}, \mathbf{k}+\mathbf{Q}}^{\Omega-}(E)] / K, \end{aligned} \quad (\text{C10})$$

where

$$\Sigma_{\mathbf{k}, \mathbf{k}+\mathbf{Q}}^{\Omega\pm}(E) = I^2 \sum_{\mathbf{q}} \frac{n_{\mathbf{k}-\mathbf{q}}(E - t_{\mathbf{k}-\mathbf{q}})}{\Omega_{\mathbf{q}}^{\pm}(E - t_{\mathbf{k}-\mathbf{q}})}. \quad (\text{C11})$$

APPENDIX D: RENORMALIZATIONS OF THE ORDERED MOMENT AND MAGNON FREQUENCY

To investigate the magnon spectrum of an antiferromagnet in model (2), we calculate the retarded Green's function of spin deviation operators in the local coordinate system

$$\Gamma_{\mathbf{q}}(\omega) = \langle\langle b_{\mathbf{q}} | b_{\mathbf{q}}^\dagger \rangle\rangle_{\omega}, \quad \bar{\Gamma}_{\mathbf{q}}(\omega) = \langle\langle b_{-\mathbf{q}}^\dagger | b_{\mathbf{q}}^\dagger \rangle\rangle_{\omega}. \quad (\text{D1})$$

Writing down the equation of motion we derive [cf. the calculations for $l=0$ (Ref. 39)]

$$\Gamma_{\mathbf{q}}(\omega) = \frac{\omega + C_{\mathbf{q}-\omega}}{(\omega - C_{\mathbf{q}\omega})(\omega + C_{\mathbf{q}-\omega}) + D_{\mathbf{q}\omega}^2}, \quad (\text{D2})$$

$$\bar{\Gamma}_{\mathbf{q}}(\omega) = \frac{D_{\mathbf{q}\omega}}{(\omega - C_{\mathbf{q}\omega})(\omega + C_{\mathbf{q}-\omega}) + D_{\mathbf{q}\omega}^2}, \quad (\text{D3})$$

where

$$\begin{aligned} C_{\mathbf{q}\omega} &= S(J_{\mathbf{Q}+\mathbf{q},\omega}^{\text{tot}} + J_{\mathbf{q}\omega}^{\text{tot}} - 2J_{\mathbf{Q}0}^{\text{tot}}) + [I] \sum_{\mathbf{p}} [C_{\mathbf{p}} \Phi_{\mathbf{p}\mathbf{q}\omega}^{\text{AFM}} \\ &\quad - (C_{\mathbf{p}} - D_{\mathbf{p}}) \Phi_{\mathbf{p}00}^{\text{AFM}} + \phi_{\mathbf{p}\mathbf{q}\omega}^+ + \phi_{\mathbf{p}\mathbf{q}\omega}^-] \\ &\quad + \sum_{\mathbf{p}} [(2J_{\mathbf{Q}} + 2J_{\mathbf{q}-\mathbf{p}} - 2J_{\mathbf{p}} - J_{\mathbf{Q}+\mathbf{q}} - J_{\mathbf{q}}) \langle b_{\mathbf{p}}^{\dagger} b_{\mathbf{p}} \rangle \\ &\quad - 2J_{\mathbf{p}} \langle b_{-\mathbf{p}} b_{\mathbf{p}} \rangle], \quad (\text{D4}) \\ D_{\mathbf{q}\omega} &= D_{\mathbf{q}-\omega} = S(J_{\mathbf{q}\omega}^{\text{tot}} - J_{\mathbf{Q}+\mathbf{q},\omega}^{\text{tot}}) + [I] \sum_{\mathbf{p}} D_{\mathbf{p}} \Phi_{\mathbf{p}\mathbf{q}\omega}^{\text{AFM}} \\ &\quad + \sum_{\mathbf{p}} [(J_{\mathbf{Q}+\mathbf{q}} - J_{\mathbf{q}}) \langle b_{\mathbf{p}}^{\dagger} b_{\mathbf{p}} \rangle - 2J_{\mathbf{q}-\mathbf{p}} \langle b_{-\mathbf{p}} b_{\mathbf{p}} \rangle]. \end{aligned}$$

The $s-f$ exchange contributions of the first order in $1/2S$ correspond to the RKKY approximation

$$J_{\mathbf{q}\omega}^{\text{tot}} = J_{\mathbf{q}} + I^2 [I] \sum_{\mathbf{k}} \frac{n_{\mathbf{k}} - n_{\mathbf{k}-\mathbf{q}}}{\omega + t_{\mathbf{k}} - t_{\mathbf{k}-\mathbf{q}}} \quad (\text{D5})$$

the second summand in Eq. (D5) being the ω -dependent RKKY indirect exchange interaction. The function Φ , which determines the second-order corrections, is given by

$$\Phi_{\mathbf{p}\mathbf{q}\omega}^{\text{AFM}} = (\phi_{\mathbf{p}\mathbf{q}\omega}^+ - \phi_{\mathbf{p}\mathbf{q}\omega}^-) / \omega_{\mathbf{p}}, \quad (\text{D6})$$

$$\phi_{\mathbf{p}\mathbf{q}\omega}^{\pm} = I^2 \sum_{\mathbf{k}} \frac{n_{\mathbf{k}}(1 - n_{\mathbf{k}+\mathbf{p}-\mathbf{q}}) + N(\pm \omega_{\mathbf{p}})(n_{\mathbf{k}} - n_{\mathbf{k}+\mathbf{p}-\mathbf{q}})}{\omega + t_{\mathbf{k}} - t_{\mathbf{k}+\mathbf{p}-\mathbf{q}} \mp \omega_{\mathbf{p}}} \quad (\text{D7})$$

(note that $\phi_{\mathbf{p}\mathbf{q}\omega}^+ = -\phi_{\mathbf{p}\mathbf{q}-\omega}^-$), $\omega_{\mathbf{p}}$ is the magnon frequency to zeroth order in I and $1/2S$ given by Eq. (A4), the terms in Eq. (D4), which contain the spin-deviation correlation functions, describe the magnon anharmonicity. Expression (D2) is valid also for a ferromagnet ($\mathbf{Q}=0$) provided that q is not too small, cf. Ref. 40; such an approximation is sufficient to treat the Kondo divergences.

We have to take into account singular $s-f$ contributions to the averages in Eq. (D4). These are due to the zero-point magnon damping and are obtained by using the spectral representation for the Green's functions (D2), (D3) in the RKKY approximation.⁹ Since $\text{Im}J_{\mathbf{q}\omega}^{\text{tot}} \sim \omega$ ($|\omega| \ll E_F$) the corresponding integral over frequency contains logarithmic Kondo-like divergences that are smeared by spin dynamics [note that scattering corrections to the damping, which are described by the function (D6), do not contribute the logarithmic terms]. We derive

$$\delta \left\{ \begin{array}{l} \langle b_{\mathbf{q}}^{\dagger} b_{\mathbf{q}} \rangle \\ \langle b_{-\mathbf{q}} b_{\mathbf{q}} \rangle \end{array} \right\} = \frac{S}{2} [I] (\Phi_{\mathbf{q}00}^{\text{AFM}} \pm \Phi_{\mathbf{q}+\mathbf{Q}00}^{\text{AFM}}) \quad (\text{D8})$$

for an antiferromagnet and

$$\delta \langle b_{\mathbf{q}}^{\dagger} b_{\mathbf{q}} \rangle = S [I] \Phi_{\mathbf{q}00}^{\text{FM}} \quad (\text{D9})$$

for a ferromagnet with

$$\Phi_{\mathbf{p}\mathbf{q}\omega}^{\text{FM}} = I^2 \sum_{\mathbf{k}} \frac{n_{\mathbf{k}}(1 - n_{\mathbf{k}+\mathbf{p}-\mathbf{q}}) + N(\omega_{\mathbf{p}})(n_{\mathbf{k}} - n_{\mathbf{k}+\mathbf{p}-\mathbf{q}})}{(\omega + t_{\mathbf{k}} - t_{\mathbf{k}+\mathbf{p}-\mathbf{q}} - \omega_{\mathbf{p}})^2}. \quad (\text{D10})$$

Expressions (D8), (D9) determine also the singular correction to the (sublattice) magnetization

$$\delta \bar{S} / S = -\frac{1}{S} \sum_{\mathbf{q}} \delta \langle b_{\mathbf{q}}^{\dagger} b_{\mathbf{q}} \rangle = -[I] \sum_{\mathbf{q}} \Phi_{\mathbf{q}00}^{\text{FM,AFM}}. \quad (\text{D11})$$

Collecting all the singular $s-f$ contributions to the pole of Eq. (D2) and taking into account the relation

$$\sum_{\mathbf{p}} J_{\mathbf{p}+\mathbf{k}} \Phi_{\mathbf{p}\mathbf{q}\omega} \simeq \sum_{\mathbf{p}} J_{\mathbf{p}+\mathbf{k}-\mathbf{q}} \Phi_{\mathbf{p}00} \sim I^2 \langle J_{\mathbf{k}-\mathbf{q}} \rangle_{t_{\mathbf{k}}=t_{\mathbf{k}-\mathbf{q}}=0} \ln \frac{D}{\omega}, \quad (\text{D12})$$

which holds to logarithmic accuracy, we derive for the singular correction

$$\begin{aligned} \delta(\omega_{\mathbf{q}}^{\text{AFM}})^2 &\equiv 2\omega_{\mathbf{q}} \delta\omega_{\mathbf{q}}^{\text{AFM}} = -R \sum_{\mathbf{p}} [2\omega_{\mathbf{q}}^2 + 4S^2(J_{\mathbf{Q}+\mathbf{q}} + J_{\mathbf{q}} \\ &\quad - 2J_{\mathbf{Q}})(J_{\mathbf{p}} + J_{\mathbf{Q}+\mathbf{p}} - J_{\mathbf{Q}+\mathbf{q}-\mathbf{p}} - J_{\mathbf{q}-\mathbf{p}})] \Phi_{\mathbf{p}00}^{\text{AFM}} \end{aligned} \quad (\text{D13})$$

with $R = [I]$.

In the case of a ferromagnet ($\mathbf{Q}=0$), the term $\phi_{\mathbf{p}\mathbf{q}\omega}^+ + \phi_{\mathbf{p}\mathbf{q}\omega}^-$ (which is odd in ω) yields a contribution to the pole of Eq. (D2) and we have

$$\delta\omega_{\mathbf{q}}^{\text{FM}}(\omega) = -2RS \sum_{\mathbf{p}} (2J_{\mathbf{p}} - 2J_{\mathbf{q}-\mathbf{p}} + J_{\mathbf{q}} - J_0 + \omega/2S) \Phi_{\mathbf{p}00}^{\text{FM}}, \quad (\text{D14})$$

$$\delta\omega_{\mathbf{q}}^{\text{FM}} = \delta\omega_{\mathbf{q}}^{\text{FM}}(\omega_{\mathbf{q}}) = -4RS \sum_{\mathbf{p}} (J_{\mathbf{p}} + J_{\mathbf{q}} - J_{\mathbf{q}-\mathbf{p}} - J_0) \Phi_{\mathbf{p}00}^{\text{FM}}. \quad (\text{D15})$$

Expression (D15) can be represented as

$$\delta\omega_{\mathbf{q}} / \omega_{\mathbf{q}} = 2(1 - \alpha_{\mathbf{q}}) \delta \bar{S} / S \quad (\text{D16})$$

with $\alpha_{\mathbf{q}}$ given by Eq. (19).

For an antiferromagnet in the nearest-neighbor approximation ($J_{\mathbf{Q}+\mathbf{q}} = -J_{\mathbf{q}}$) we obtain from Eq. (D13)

$$\delta\omega_{\mathbf{q}} / \omega_{\mathbf{q}} = \delta \bar{S} / S, \quad (\text{D17})$$

so that, in contrast with the PM and the FM cases, an explicit dependence on the parameter $k_F d$ is absent. Note that the results (D16), (D17) differ from those of Ref. 13 since only corrections arising from the static correlation functions were taken into account in that paper.

The calculations of the magnon spectrum in the Coqblin-Schrieffer model for the FM and AFM1 cases are performed in a similar way by considering the Green's functions

$$\Gamma_{\mathbf{q}}^{MM'}(\omega) = \langle \langle \hat{X}_{\mathbf{q}}^{M'M} | \hat{X}_{-\mathbf{q}}^{MM'} \rangle \rangle_{\omega},$$

$$\bar{\Gamma}_{\mathbf{q}}^{MM'}(\omega) = \langle \langle \hat{X}_{\mathbf{q}}^{-M', -M} | \hat{X}_{-\mathbf{q}}^{MM'} \rangle \rangle_{\omega} \quad (\text{D18})$$

for $M' = S$. The results differ from Eqs. (D2), (D3) by the replacement $[l] \rightarrow 1$ in Eq. (D5) and $[l] \rightarrow N/2$ in Eq. (D4).

According to Eq. (9), the magnetization of a ferromagnet is determined by

$$\bar{S}/S = 1 - Nn_{-}, \quad n_{-} = \sum_{\mathbf{q}} \langle X_{-\mathbf{q}}^{MS} X_{\mathbf{q}}^{SM} \rangle, \quad (\text{D19})$$

where the average in the right-hand side does not depend on M for $M < S$. Then we obtain

$$\delta \bar{S}/S = -\frac{N}{2} \sum_{\mathbf{q}} \Phi_{\mathbf{q}00}^{\text{FM}}, \quad \delta \omega_{\mathbf{q}} = \frac{N}{2} \delta \omega_{\mathbf{q}}^{\text{FM}}. \quad (\text{D20})$$

The sublattice magnetization in the AFM1 case is given by

$$\bar{S}/S = 1 - (N-2)n_{-} - 2n_{-S} \quad (\text{D21})$$

with

$$n_{-} = \sum_{\mathbf{q}} \langle \hat{X}_{-\mathbf{q}}^{MS} \hat{X}_{\mathbf{q}}^{SM} \rangle \quad (-S < M < S), \quad (\text{D22})$$

$$n_{-S} = \sum_{\mathbf{q}} \langle \hat{X}_{-\mathbf{q}}^{-SS} \hat{X}_{\mathbf{q}}^{S, -S} \rangle$$

After cumbersome calculations we derive

$$\delta \bar{S}/S = -\frac{N-2}{2} \sum_{\mathbf{q}} \Phi_{\mathbf{q}00}^{\text{FM}}(\omega_{\mathbf{p}}^{\text{FM}} \rightarrow \omega_{\mathbf{p}}^{(f)})$$

$$- \sum_{\mathbf{q}} \Phi_{\mathbf{q}00}^{\text{AFM}}(\omega_{\mathbf{p}}^{\text{AFM}} \rightarrow \omega_{\mathbf{p}}^{(a)}), \quad (\text{D23})$$

$$\delta \omega_{\mathbf{q}}^{(f)} = \frac{N-2}{N} \delta \omega_{\mathbf{q}}^{\text{FM}}(J_{\mathbf{p}} \rightarrow J_{\mathbf{p}}^{(2)}) + \delta(\omega_{\mathbf{q}}^{\text{AFM}})^2 / (NC_{\mathbf{q}}), \quad (\text{D24})$$

$$\delta(\omega_{\mathbf{q}}^{(a)})^2 = \frac{2}{N} \delta(\omega_{\mathbf{q}}^{\text{AFM}})^2 (\omega_{\mathbf{p}}^{\text{AFM}} \rightarrow \omega_{\mathbf{p}}^{(a)}) + 2 \frac{N-2}{N} C_{\mathbf{q}}$$

$$\times \delta \omega_{\mathbf{q}}^{\text{FM}}(\omega = \omega_{\mathbf{q}}^{(a)}, J_{\mathbf{p}} \rightarrow J_{\mathbf{p}}^{(2)})$$

with $R = N/2$ in Eqs. (D14), (D13).

In the AFM2 case we have to put in Eq. (D18) $M < 0, M' > 0$. Then we have

$$\bar{S} = (\bar{S})_0 - \begin{cases} (S+1/2)^2 n_{-}, & N \text{ even} \\ S(S+1)n_{-} + (S+1)\delta n_0, & N \text{ odd.} \end{cases} \quad (\text{D25})$$

where $(\bar{S})_0$ is given by Eq. (A11), the average

$$n_{-} = \sum_{\mathbf{q}} \langle \hat{X}_{-\mathbf{q}}^{M, M'} \hat{X}_{\mathbf{q}}^{M', M} \rangle$$

does not depend on M, M' for $M' > 0, M < 0$, and δn_0 is the fluctuation correction to n_0 . Restricting ourselves for simplicity to the case of even N , which corresponds to a realistic situation for f ions, we obtain

$$\delta \bar{S}/S = -\sum_{\mathbf{q}} \Phi_{\mathbf{q}00}^{\text{AFM}}(\omega_{\mathbf{p}}^{\text{AFM}} \rightarrow \omega_{\mathbf{p}}^{(a)}), \quad (\text{D26})$$

$$\delta \omega_{\mathbf{q}}^{(a)} = \frac{2}{N} \delta \omega_{\mathbf{q}}^{\text{AFM}}(\omega_{\mathbf{p}}^{\text{AFM}} \rightarrow \omega_{\mathbf{p}}^{(a)}). \quad (\text{D27})$$

Thus the singular corrections to the sublattice magnetization and magnon frequency do not contain the factor of N in this case.

*Electronic address: Mikhail.Katsnelson@usu.ru

¹G. R. Stewart, Rev. Mod. Phys. **56**, 755 (1987).

²N. B. Brandt and V. V. Moshchalkov, Adv. Phys. **33**, 373 (1984); V. V. Moshchalkov and N. B. Brandt, Usp. Fiz. Nauk **149**, 585 (1986).

³D. T. Adroya and S. K. Malik, J. Magn. Magn. Mater. **100**, 126 (1991), and references therein.

⁴P. Fulde, J. Keller, and G. Zwicknagl, *Solid State Physics: Advances in Research and Applications*, edited by F. Seitz *et al.* (Academic, New York, 1988), Vol. 41, p. 1.

⁵G. Zwicknagl, Adv. Phys. **41**, 203 (1992).

⁶P. A. Lee, T. M. Rice, J. W. Serene, L. J. Sham, and J. W. Wilkins, Comments Condens. Matter Phys. **12**, 99 (1986).

⁷C. Lacroix, J. Magn. Magn. Mater. **100**, 90 (1991).

⁸S. Doniach, Physica B & C **91**, 231 (1977).

⁹V. Yu. Irkhin and M. I. Katsnelson, Fiz. Tverd. Tela **30**, 2273 (1988); Z. Phys. B **75**, 67 (1989).

¹⁰V. Yu. Irkhin and M. I. Katsnelson, Z. Phys. B **82**, 77 (1991).

¹¹V. Yu. Irkhin and M. I. Katsnelson, Fiz. Met. Metalloved. **71** (1), 16 (1991) [Phys. Met. Metallogr. **71**, 13 (1991)]; S. V. Vonsovsky, V. Yu. Irkhin, and M. I. Katsnelson, Physica B **163**, 321 (1990).

¹²S. V. Vonsovsky, V. Yu. Irkhin, and M. I. Katsnelson, Physica B **171**, 135 (1991).

¹³V. Yu. Irkhin and M. I. Katsnelson, J. Phys.: Condens. Matter **4**, 9661 (1992).

¹⁴M. B. Maple *et al.*, J. Low Temp. Phys. **95**, 225 (1994); **99**, 223 (1995); J. Phys.: Condens. Matter **8**, 9773 (1996).

¹⁵K. Umeo, H. Kadomatsu, and T. Takabatake, J. Phys.: Condens. Matter **8**, 9743 (1996).

¹⁶F. Steglich *et al.*, J. Phys.: Condens. Matter **8**, 9909 (1996).

¹⁷B. Andraka and A. M. Tsvetlik, Phys. Rev. Lett. **67**, 2886 (1991); A. M. Tsvetlick and M. Reizer, Phys. Rev. B **48**, 9887 (1993).

¹⁸D. L. Cox and M. Jarrell, J. Phys.: Condens. Matter **8**, 9825 (1996).

¹⁹P. Coleman, L. B. Ioffe, and A. M. Tsvetlik, Phys. Rev. B **52**, 6611 (1995).

²⁰V. Yu. Irkhin and M. I. Katsnelson, Pis'ma Zh. Eksp. Teor. Fiz. **49**, 550 (1989); Phys. Lett. A **150**, 47 (1990).

²¹P. Nozieres and A. Blandin, J. Phys. (Paris) **41**, 193 (1980).

²²A. M. Tsvetlick and P. B. Wiegmann, Adv. Phys. **32**, 745 (1983).

²³B. Coqblin and J. R. Schrieffer, Phys. Rev. **185**, 847 (1969).

²⁴J. R. Schrieffer, J. Appl. Phys. **38**, 1143 (1967).

²⁵L. L. Hirst, Z. Phys. **244**, 230 (1971); Int. J. Magn. **2**, 213 (1972); Adv. Phys. **21**, 295 (1972).

- ²⁶V. Yu. Irkhin and Yu. P. Irkhin, Zh. Eksp. Teor. Fiz. **107**, 616 (1995).
- ²⁷H. Brooks, Phys. Rev. **58**, 909 (1940).
- ²⁸S. V. Vonsovsky, A. V. Trefilov, and M. I. Katsnelson, Phys. Met. Metallogr. **76**, 247 (1993); **76**, 343 (1993).
- ²⁹D. M. Newns and N. Read, Adv. Phys. **36**, 799 (1987).
- ³⁰N. E. Bickers, Rev. Mod. Phys. **59**, 845 (1987).
- ³¹P. W. Anderson, J. Phys. C **3**, 2346 (1970).
- ³²T. Moriya, *Spin Fluctuations in Itinerant Electron Magnetism* (Springer, Berlin, 1985).
- ³³V. Yu. Irkhin and M. I. Katsnelson, Z. Phys. B **70**, 371 (1988).
- ³⁴E. Abrahams, J. Magn. Magn. Mater. **63-64**, 235 (1987); T. Yanagisawa, J. Phys. Soc. Jpn. **60**, 3449 (1991).
- ³⁵G. Broholm, J. K. Kjems, G. Aeppli, Z. Fisk, J. L. Smith, S. M. Shapiro, G. Shirane, and H. R. Ott, Phys. Rev. Lett. **58**, 917 (1987).
- ³⁶V. Yu. Irkhin and M. I. Katsnelson, Usp. Fiz. Nauk **164**, 705 (1994).
- ³⁷P. Fulde and M. Loewenhaupt, Adv. Phys. **34**, 589 (1986).
- ³⁸T.-S. Kim and D. L. Cox, Phys. Rev. B **54**, 6494 (1996).
- ³⁹V. Yu. Irkhin and M. I. Katsnelson, Phys. Rev. B **53**, 14008 (1996).
- ⁴⁰M. I. Auslender and V. Yu. Irkhin, Z. Phys. B **56**, 301 (1984).